M-alpha2/delta promotes myonuclear positioning and association with the sarcoplasmic-reticulum

Adriana Reuveny[1], Marina Shnayder[1], Dana Lorber[1], Shuoshuo Wang[2] and Talila Volk*[1]

1 - Department of Molecular Genetics, Weizmann Institute

2 – Current address: Institute of Systems Genetics (ISG), New York University School of Medicine, NYU Langone Health, New York, United States.

* - Corresponsing author

Abstract

The cytoplasm of striated myofibers contains a large number of membrane organelles, including sarcoplasmic reticulum (SR), T-tubules, and the nuclear membrane. These organelles maintain a characteristic juxtaposition, that appears to be essential for efficient inter-membranous exchange of RNA, proteins, and ions. We found that the membrane associated muscle-specific alpha2/delta subunit of the Ca^{++} channel complex (Ma2/d) localizes to the SR and T-tubules, and accumulates at the myonuclear surfaces. Furthermore, *Ma2/d* mutant larval muscles exhibt nuclear positioning defects, disruption of the nuclear-SR juxta positioning, as well as impaired larval locomotion. Ma2/d localization at the nuclear membrane depends on the proper function of the Nesprin orthologue Msp300, and the BAR domain protein Amphiphysin (Amph). Importantly, live imaging of muscle contraction in intact larvae indicated altered distribution of Sarco/Endoplamic Reticulum Ca^{2+}- ATPase (SERCA) around the myonuclei of *Ma2/delta* mutant larvae. Co-immunoprecipitation analysis supports association between Ma2/d and Amphiphysin, and indirectly with Msp300. We therefore suggest that Ma2/d in association with Msp300 and Amph mediate interactions between the SR and the nuclear membrane.

Introduction

Fully differentiated skeletal muscle fibers are multinucleated, elongated cells with highly ordered cytoplasm, essential for efficient muscle contraction and organismal movement. Muscle nuclei are positioned evenly along the contractile axis, and are typically located between the myofilament compartment and the plasma membrane, in close proximity to T-tubule membrane indentations, and the sarcoplasmic reticulum (SR) (Cadot et al., 2015; Folker and Baylies, 2013; Gundersen and Worman, 2013). Despite significant cytoplasmic flow produced by muscle contractile/relaxation waves the relative position of myonuclei, T-tubules, and SR remains robust in mature muscle fibers, implicating certain connectivity between these organelles. Importantly, the maintenance of myonuclei position and shape appears to be essential for muscle function, as their abnormal aggregation is observed in a variety of muscle diseases, including Emery Dreifuss Muscular Dystrophy (EDMD) (Muchir and Worman, 2007; Puckelwartz and McNally, 2011; Puckelwartz et al., 2009; Zhang et al., 2007), cardiac diseases, Centronuclear Myopathy (CNM) (Jungbluth and Gautel, 2014) and others. The mechanisms controlling myonuclear position relative to SR are largely unknown.

Recent studies in model organisms, including *Drosophila*, zebrafish, *C. elegans,* and mice identified a number of molecular components required for nuclear positioning in muscle fibers. These include Nesprins (Elhanany-Tamir et al., 2012; Fischer et al., 2004; Starr and Han, 2002; Technau and Roth, 2008; Volk, 1992), SUN-domain proteins (Cain et al., 2014; Kracklauer et al., 2007; McGee et al., 2006), Lamins (Bank et al., 2011; Dialynas et al., 2012;

Dialynas et al., 2010; Mattout et al., 2011), Amphiphysin (D'Alessandro et al., 2015; Mathew et al., 2003; Razzaq et al., 2001), Myotubularin (Ribeiro et al., 2011; Yu et al., 2012), and microtubule-binding proteins, Map7 (also known as Esconsin) (Metzger et al., 2012), Kinesin (Folker et al., 2014), Dynein (Folker et al., 2012; Schulman et al., 2014), ACF7/Shot (Wang et al., 2015), and EB1 (Wang et al., 2015). Whereas proteins such as Esconsin, Kinesin, Dynein, Klar (a *Drosophila* Nesprin-like protein), and Klaroid (a *Drosophila* SUN domain protein) appear to mediate nuclear transport during myotube development, contributing to the initial nuclear position, others including Msp300, Amphyphisin, Lamins, Myotubularin, Shot (a Drosophila ACF7-like protein) and EB1 are required in fully differentiated muscle fibers (Volk, 2012). Hence, their function correlates with the establishment of the sarcomere structures and the onset of muscle contraction. Although the functional data regarding these gene products has been obtained primarily from model organisms, the structural similarity with their mammalian orthologs is expected to uncover basic mechanisms regulating organelles positioning within striated, contractile muscle fibers.

MSP-300, the *Drosophila* ortholog gene of mammalian Nesprin 1 (SYNE 1) and Nesprin 2 (SYNE 2), produces isoforms with KASH domain (a domain inserted into the outer myonuclear membrane), and isoforms lacking the KASH domain, which localize at distinct cytoplasmic domains, including along perinuclear microtubule, Z-discs, and post-synaptic buttons (Elhanany-Tamir et al., 2012; Morel et al., 2014; Packard et al., 2015). Msp300 labeling is often observed as thin filaments with elastic properties, which link the nucleus with Z-discs, and postsynaptic buttons. In *Msp300* homozygous

mutant larvae the myonuclei aggregate and dissociate from the perinuclear microtubule network, leading to defective muscle function (Elhanany-Tamir et al., 2012). Amphiphysin (also known as BIN1) (Amph), an N-terminal bar-domain protein with a C-terminal SH3 motif, is required for membrane curvature during endocytosis and recycling, as well as for T-tubules biogenesis in *Drosophila* muscles (Lee et al., 2002; Mathew et al., 2003; Razzaq et al., 2001; Royer et al., 2013). Recent findings indicated that in cultured differentiating myotubes, as well as in *C. elegans* epithelial seam cells, Amph is required for nuclear position (Adam et al., 2015; Caldwell et al., 2014; D'Alessandro et al., 2015; Falcone et al., 2014). Amph interactions with N-WASP, and with ANC-1 (*C. elegans* Nesprin 1 ortholog), as well as with CLIP 170 have been shown to be important for myonuclear position.

Using *Drosophila* larval muscles to uncover molecular processes promoting nuclear positioning in muscle fibers, we identified Ma2/d. The *Ma2/d* gene is a member of a family of three genes in *Drosophila*, *straight jacket* (stj) (Ly et al., 2008; Neely et al., 2010; Tian et al., 2015), CG4587 and CG42817, and four genes in mammals all of which share a trans-membrane, or GPI linked domain, and von Willebrand factor A (VWA) domain with Ca++ binding motif (Dolphin, 2012; Dolphin, 2013). Previous studies demonstrated that alpha2/delta proteins form part of the voltage-gated calcium channel complex, which allows Ca^{2+} entry into the cell during membrane depolarization. The alpha2/delta proteins function as auxiliary components to modulate the extent of Ca^{2+} signaling in different tissues (Dolphin, 2012). In both vertebrates and invertebrates the alpha2/delta subunit physically interacts with the Ca^{2+} channel core protein $C\alpha v1$ or $C\alpha v2$ and regulates their

levels at the plasma membrane, thereby indirectly controlling the extent of Ca^{2+} signaling (D'Arco et al., 2015). Clearly, the alpha2/delta subunit has additional, Ca-channel-independent roles in various cell types including muscles. In *Drosophila,* it is associated with endosomes, autophagosomes and lysosomal fusion (Tian et al., 2015). In vertebrates, alpha2/delta proteins are involved in the development and migration of myotubes independently of their role in the muscle calcium channel complex (Garcia et al., 2008), and in addition they couple between T-tubules and the sarcoplasmic reticulum (Block et al., 1988). In neurons alpha2/delta promotes synapse formation in response to Thrombospondin, or to Gabapentin, an analgesic component (Eroglu et al., 2009). Because Thrombospondin is essential for proper muscle development, both in *Drosophila* and zebrafish (Subramanian and Schilling, 2014; Subramanian et al., 2007), we set up to investigate the role of alpha2/delta in *Drosophila* muscle development.

Our results imply that Ma2/d contributes predominantly for nuclear association with the SR, as well as for nuclear position in striated muscles. Ma2/d localizes along the T-tubules, SR, and accumulates along the nuclear membrane. Larval muscles lacking functional Ma2/d exhibit abnormal myonuclear position, disruption of nuclear-SR juxta-position, and slower locomotive activity.

Results

Ma2/d *is localized along the T-tubules, SR, and at the nuclear membrane*

To reveal the subcellular distribution of Ma2/d in muscle fibers we produced flies expressing Ma2/d-GFP by fusing full length Ma2/d with GFP at its most

C-terminal sequence (Figure 1 upper panel), and expressed it using a muscle-specific *Mef2-GAL4* driver. Importantly, this overexpression did not affect normal development and flies expressing Ma2/d-GFP were viable. Co-labeling of GFP with Amphiphysin (Amph) indicated numerous sites of elongated structures labeled with Ma2/d-GFP and decorated with punctate Amph, corresponding to T-tubules (Fig 1A-A'', empty arrows). In addition, Amph-positive dots around the nuclear membrane often overlapped Ma2/d-GFP (Fig 1 A-A''', arrows). Furthermore, Ma2/d-GFP labeling surrounded each of the myonuclei, and corresponded to the sarcoplasmic reticulum (SR), as indicated by overlap labeling with SERCA (Fig 1 C-C''). To discriminate between plasma membrane versus SR membranes, larvae were labeled with a recently described plasma membrane fluorescent dye, "membrane-binding fluorophore-cystein-lysine-palmitoyl" (mCLING), prior to fixation (Revelo and Rizzoli, 2016), and then fixed and labeled with GFP. mCLING is expected to label the plasma membrane, including T-tubules surfaces, but not the SR membrane. Consistent with localization of Ma2/d-GFP in the SR, we detected GFP labeling surrounding the myonuclei that was mCLING-negative (Fig 1 B-B'', empty arrows). In addition, Ma2/d-GFP labeled structures that were closely related to mCLING and accumulated at the myonuclear periphery, presumably labeling points of intersection between T-tubules and the SR or nuclear membrane (Fig 1 B-B'', and B''',B'''', filled arrows). Co-labeling of anti GFP with SERCA revealed overlap localization around the myonuclei (Fig 1 C-C'' filled arrows), as well as along the T-tubules associated SR (Fig 1 C-C'', empty arrows). It was concluded that Ma2/d-GFP distribution was confined to the SR, T-tubules, and to Amph-positive nuclear associated dots. Although

the Ma2/d-GFP was overexpressed by Mef2-GAL4 and might not represent endogenous levels, the overexpression did not affect viability of the larvae and flies, nor did it affect larval locomotion.

To confirm the distribution of Ma2/d in muscles, an antibody raised against a mixture of three conserved peptides (each fused to KLH) of Ma2/d extracellular domain was produced (the epitopes and peptides are indicated in Fig 2 upper panel). Specificity of the antibody was verified by its positive reactivity with ectopically expressed Ma2/d-GFP in the wing imaginal disc (Supp. Fig S1 A-C) and by Western blot (Supp Fig S1 D, E). The anti Ma2/d antibody exhibited overlapping distribution with the muscle-driven Ma2/d-GFP (Fig 2 A-A'') confirming its distribution at the T-tubules, SR, and nuclear periphery. Furthermore, the anti Ma2/d antibody exhibited overlapped distribution with SERCA at the perinuclear region, confirming their co-localization at this region (Fig 2 B-B''). Collectively, it was concluded that Ma2/d localizes to T-tubules, SR, and the nuclear periphery.

Production of Ma2/d mutant larvae

We performed knockout of the *Ma2/d* gene by a P-element excision of a transgene insertion EPgy2^{EY2EY09750} located at the first intron of the gene. Sequence analysis of the genomic region following the P element excision indicated a deletion and rearrangement within the first intron, 5' to the P element, extending to the end of the first exon, presumably interfering with its proper splicing (Supp. Fig S2). Because an additional methionine residing in the third exon might provide a translation start site, the mutant larvae were expected to express a truncated Ma2/d protein of ~80kDa, which should be

still recognized by the antibody, however, such protein is not expected to be functional due to the lack of a signal peptide. Adult flies mutants for this allele were homozygous lethal, and in addition were lethal in trans over a chromosomal deficiency (Df(2L)BSC293) that removed the corresponding genomic region, confirming that lethality is due to *Ma2/d* destruction. The homozygous mutant larvae carrying the heteroallelic combination of *Ma2/d /Df(2L)BSC293* were further analyzed to reveal the contribution of *Ma2/d* for proper development of the somatic musculature.

Western analysis with the anti Ma2/d antibody recognized a specific band in the protein extract of larvae expressing the Ma2/d-GFP (driven by muscle-specific *Mef2-GAL4*) of the expected 170kDa size (140kDa of full length Ma2/delta fused to GFP), and this band was also reactive with anti GFP antibody (Fig S1 E, left panel), confirming antibody specificity. The anti GFP also recognized a 50kDa band by Western analysis, representing the cleaved delta subunit fused to GFP (Fig S1 E, left panel). This band was not reactive with the anti Ma2/d antibody, since it was raised against sequences located N-terminally to the cleavage site (Figure S1, D). Importantly, whereas the anti Ma2/d recognized a protein band of 140kDa in a protein extract of wild type larvae it reacted with a protein band of ~80kDa in *Ma2/d* mutant larvae (Fig S1, right panel). This band apparently represents the truncated Ma2/d mutant protein. Furthermore, staining of the *Ma2/d* mutant larvae with anti Ma2/d did not show specific staining (Fig 2 C,D), implicating that the truncated protein observed by the Western was not localized properly, possibly because it lacks the signal peptide. We concluded that the hetero-allelic combination of EPgy2$\Delta^{EY2EY09750}$/ Df(2L)BSC293 mutant larvae lack

functional Ma2/d and therefore further analyzed the phenotype of larvae carrying this allelic combination (refers to *Ma2/d* in all figures).

Ma2/d mutant muscles exhibit abnormal nuclear position

The muscles of the *Ma2/d* mutant larvae exhibited abnormal nuclear positioning phenotype where the myonuclei were significantly closer to each other and often created small aggregates (Fig 3 A-B"', C, and also see Supplementary Fig S3 indicating aberrant myonuclear position following knockdown of *Ma2/d* with RNAi driven by Mef2-GAL4 driver). Of note, the *M2/d* mutant muscle length remained unchanged (Fig S3). This phenotype was reminiscent of that observed in the LINC complex mutants *Msp300, klar and koi,* although it was less severe (Elhanany-Tamir et al., 2012). Interestingly, the typical perinuclear distribution of Msp300, which normally forms a ring surrounding each myonucleus was altered and the protein often aggregated at the nuclear vicinity (Figure 3 A, B (arrow)). In contrast, Msp300 localization appears normal at the Z-bands. We therefore concluded that M2/d is required for promoting Msp300 nuclear localization as well as for proper myonuclear position.

To reveal the physiological requirement for *Ma2/d* we performed a larval locomotion assay for the mutant larvae as previously described (Elhanany-Tamir et al., 2012). The *Ma2/d* mutant larvae were 41% slower relative to wild type larvae (Fig 3D; $p<0.005$; N=7), implying an important contribution of Ma2/d for muscle function.

Ma2/d mutant muscles exhibit defects in the nuclear-SR association

Further analysis indicated that SERCA, which marks both, the SR along the T-tubules, as well as the SR associated with the myonuclei, is significantly reduced at the perinuclear vicinity, and its distribution is abnormal, forming small aggregates in the *Ma2/d* mutant larvae (Fig 4 A-B'). We quantified SERCA peak fluorescence intensity at the nuclear periphery relative to background levels at the nuclear interior along the nuclear meridian (see example in Fig. 4 D). A significant reduction in SERCA levels at the nuclear periphery (normalized to background levels) was observed in *Ma2/d* mutant myonuclei relative to control (Fig 4 E; *t* test p=9E-18). WT group: included n=40 nuclei, measured from 3 larvae, in 10 different muscle no. 6; Mutant group: included n=29 nuclei analyzed from 3 larvae, from 8 different muscle no. 6). Importantly, a concomitant measurement of Lamin C fluorescence peaks at the nuclear membrane (normalized to background levels) at the same optical section, indicated that Lamin C levels did not change significantly in the *Ma2/d* mutant myonuclei, relative to control (Fig. 4 F; *t* test p=0.3; same nuclei as above). The reduced perinuclear distribution of SERCA was also observed when we knocked down *Ma2/d* in muscles following muscle-specific expression of *Ma2/d* RNAi (Fig S3). Importantly, the reduced SERCA levels at the nuclear periphery were partially rescued by a muscle-specific expression of Ma2/d-GFP in the mutant *Ma2/d* larvae (Fig 4 C, C', D, E; *t* test p=0.001; The rescue group included n=37 nuclei, analyzed from 10 muscles from 5 distinct larvae; The mutant group was as above). Lamin C levels did not change significantly between the mutant and rescue groups (*t* test p=0.1). Of note, overexpression of Ma2/d in the mutant *Ma2/d* muscles

did not rescue SERCA levels to the extent of control muscles, possibly indicating that it is not fully active (comparison between SERCA levels in the rescue nuclei versus control indicates a significant difference, *t* test p=3E-10; the number of nuclei of the rescue and control groups are indicated above). Lamin C levels were comparable between the rescue and control groups (*t* test p=0.2). We therefore concluded that Ma2/d is required for proper SERCA distribution (representing the SR), at the vicinity of the nuclear membrane.

To further address the contribution of Ma2/d for SR-nucleus association in intact larvae, during muscle contraction we imaged immobilized live intact larvae expressing either Ma2/d GFP, or Cherry-SERCA in control muscles, or in *Ma2/d* mutant larvae, and followed their distribution during muscle contractile waves. This was performed by immobilization of live larvae expressing muscle-specific Ma2/d-GFP, or Cherry-SERCA and their imaging under the Spinning disc microscope (Fig. 5). We detect two Ma2/d-GFP-positive perinuclear structures: a tight nuclear ring (Fig 5A empty arrowhead), and an outer, wider ring (Fig. 5 A, A'' empty arrow), that forms continuity with the transverse SR along the T-tubules (Fig 5A filled arrow). Notably, thin M2/d-GFP positive threads extend between the two perinuclear rings (Fig. 5 A' white filled arrow . These threads possibly represent membrane extensions connecting the distinct SR compartments. Importantly, during the contractile wave (Fig 5 A''- A''') the two nuclear rings move together with the transverse SR-associated T-tubules (Fig 5 A filled arrowhead) and the thin membrane connections, implying their physical connectivity (see also Supp movie 1). We therefore conclude that Ma2/d-GFP forms membrane continuity between distinct SR compartments.

Next, we expressed SERCA-mCherry in muscles of wild type, and *Ma2/d* mutant larvae and followed its distribution in immobilized intact larval myofibers. Overexpression of SERCA-mCherry often forms small protein aggregates, however, the nuclear borders were clearly detected (Figure 5, B empty arrow). SERCA-mCherry is also detected along the T-tubules-associated SR (Figure 5 B, empty arrowhead). Strikingly, in *Ma2/d* mutant muscles the nuclear-associated SR marked by SERCA-mCherry showed irregularities at the perinuclear area during muscle contraction/relaxation (Figure 5 C, C'' arrow). We assume that these irregularities represent partial dissociation of the SR from the nuclear membrane, since after fixation SERCA fluorescence significantly decreased at the nuclear area of *Ma2/d* mutant larvae (Fig 4 B, E). These data suggested that the association between the SR and the nucleus was partially disrupted in *Ma2/d* mutants both in fixed, flat-opened larvae, as well as in intact, live larvae.

Amph is required for the perinuclear distribution of Ma2/d and Msp300

Amph interactions with N-WASP, ANC-1, and CLIP 170 contribute to nuclear positioning in *C. elegans* and in differentiating myofibers in culture (D'Alessandro et al., 2015; Falcone et al., 2014). We examined the contribution of Amph to nuclear position, as well as to Msp-300, and Ma2/d nuclear localization. In wild type muscles, Msp300 and Ma2/d both co-localize around the nucleus but not along the Z-bands, where Msp300 is prominent (Fig 6 A-E'). In *Amph* mutant muscles both Msp300 and Ma2/d dissociate from the myonuclear surfaces (Fig 6F-J'). *Amph* mutant myonuclei showed partial or complete dissociation of Msp300 and Ma2/d from the the perinuclear

area in 42.9% of the myonuclei; n = 46 nuclei analyzed from 6 muscles of 3 *Amph* mutant larvae. In contrast 100% of control muscles showed normal perinuclear distribution of Ma2/d and Msp300. For Ma2/d distribution n = 76 from 15 muscles analyzed from 7 larvae; for Msp300 distribution n = 65 from 12 muscles analyzed from 6 different larvae. This suggested a role for Amph in connecting both Msp300 and Ma2/d to the nuclear membrane. Despite the dissociation of Msp300 protein from the nuclear membrane in many cases it still overlaped with Ma2/d, implicating a possible association between these proteins that is Amph-independent. Consistent with previous reports the even myonuclear positioning was frequently aberrant in *Amph* mutants (Fig. 6 F-I') (Razzaq et al., 2001). Abnormal SR distribution has been previously reported in *Amph* mutant muscles (Razzaq et al., 2001). Consistent with dissociation of the SR from the nuclear membrane in *Amph* mutant muscles, we detect a nuclear dissociation of Ma2/d (Fig 6 G,G'). Furthermore, larval locomotion assay indicated that the Amph mutant larvae move slower relative to control (Supplementary Figure S4).

Reciprocally, we show that in *Msp300* mutant muscles Amph labeling at the myonuclear area is abnormal, and furthermore Ma2/d staining at the perinuclear area is absent (Fig 7 compare A-C to D-F; *Msp300* mutants nuclei: 98% showed a comlete loss of Amph around the nuclear area, 81% showed complete loss of Ma2/d around the nuclear area, and 18.6% showed partial loss of Ma2/d; number of mutant nuclei n = 118 counted from 8 muscles of 4 different mutant larvae; Control myonuclei: 100% showed normal perinuclear distribution of Ma2/d and Amph. For Ma2/d distribution n = 76 nuclei from 15 muscles from 7 different larvae; for Amph distribution n = 93

nuclei from 18 muscles from 8 larvae). In addition, both proteins were not distributed porperly along the T-tubules (Fig 7D, arrow). Since *Msp300* mutant muscles exhibit a wide range of defects in sarcomere, mitochondria, and ER exit site localization in myofibers (Elhanany-Tamir et al., 2012) it was not clear whether the abnormal distribution of Amph and Ma2/d at the nuclear periphery depended directly on Msp300.

Molecular association between Ma2/d, Amph, and Msp300

To address whether Ma2/d, Msp300, and Amph form a protein complex in the larval muscles we performed co-immunoprecipitation experiments using larvae expressing Ma2/d-GFP in muscles, and immunoprecipitated the larval protein extract with anti GFP. Of note these experiments were performed with muscles overexpressing Ma2/d-GFP (whose levels might be higher relative to endogenous levels), nevertheless it was found that Amph co-precipitated with Ma2/d-GFP in these conditions, consistent with the overlapped distribution of both proteins, and with their closely related phenotypes. We could not demonstrate co-immunoprecipitation between Ma2/d and MSP-300, possibly due to the abundance of Msp300 in sites deficient of Ma2/d (e.g. Z-bands). In addition, Immunoprecipitation with anti Msp300 revealed its co-precipitation with Amph (Fig 8 B), implying that these proteins form a protein complex.

Taken together these results suggest that Amph forms a protein complex with Ma2/d, as well as with Msp-300, however these protein complexes might be separated. Functionally, both complexes are required for nuclear positioning, as well as for perinuclear SR integrity.

Discussion

Despite their large size, muscle fibers exhibit highly ordered cytoplasm in which membrane organelles, e.g. SR, mitochondria, are localized juxtapose the outer nuclear membrane (Clark et al., 2002; Gautel and Djinovic-Carugo, 2016; Hong and Shaw, 2017). Nuclear juxtaposition is presumably essential for effective transport of mRNAs and proteins as well as for efficient ion coupling across membranous compartments. How this coupling is achieved and maintained despite the contractile nature of muscle fibers, is an important and open question. Based on our experiments we suggest that the membrane protein Ma2/d in combination with Amphiphysin and Msp300 are essential components in maintaining SR-nuclear juxta positioning during muscle contractile/relaxation waves.

We suggest that Ma2/d is a membrane component required for inter-membranous organelles connectivity through its association with Amph, and through the association of Amph with Msp300 (Fig 8 C). This proposed model is based on the phenotypic similarities shared between the three mutants affecting myonuclei position, and their association with the SR, as well as their overlapped distribution. Most notable is the aberrant position of the myonuclei, which correlates with both dispersed nuclear distribution of Msp300 and Amph in the *Ma2/d* mutant muscles. Additional evidence emerges from the co-immunoprecipitation data suggesting that Amph associates with Ma2/d, and with Msp300.

The *Drosophila* Ma2/d protein contains a trans-membrane domain and a very short cytoplasmic tail. Our data suggests that Ma2/d forms part of a protein complex that includes Amph, a protein shown previously to promote membrane curvature, e.g. in the T-tubules (Caldwell et al., 2014; Mim and Unger, 2012; Razzaq et al., 2001). Amph could directly interact with Ma2/d cytoplasmic tail or indirectly through its association with components of the Ca^{2+} channel. We favor the second option due to the short cytoplasmic tail of Ma2/d. Whereas we recognize that the addition of GFP to the cytoplasmic tail of M2/d could abnormally retain a portion of the Ma2/d-GFP at the SR, we do detect similar distribution of endogenous Ma2/d using the antibody raised against Ma2/d in larval muscles, supporting a correct localization of Ma2/d-GFP at these sites. At the vicinity of the nuclear membrane, we observed that Ma2/d-GFP positive dot-like structures corresponded to extracellular mCLING-positive accumulation, which might represent points of intersection between T-tubules (labeled with mCLING at the extracellular space) and the nuclear and/or SR membranes, (model in Fig 8C). Msp300 at the nuclear membrane might provide physical support to these contact sites through its association with Amph, and with the nuclear membrane. Furthermore, dimerization of Msp300 through its multiple spectrin repeats domain, results in the formation of elongated filaments that would enhance the connections between the two organelles as described for Msp300 connections between the muscle nuclei and the neuromuscular junction (Packard et al., 2015).

The *Msp300* gene codes for multiple protein isoforms, some of them are extremely large and either, contain or lack the KASH domain (Gramates et al., 2017). We previously reported that the multiple spectrin repeats along the Msp300 sequence provide elastic properties to the connections between the nuclear membrane and the Z-discs (Wang et al., 2015). Similarly, the association between Amph and Msp300 should provide elasticity to the connections between the SR and T-tubules membranes. Taken together, our results imply that the three proteins, namely Ma2/d, Amph, and Msp300 mediate the formation and maintenance of contacts sites between the SR and the myonuclei, presumably required to maintain SR-nuclear juxta positioning in contractile muscles.

In vertebrates, the auxiliary subunit alpha-2/delta protein contributes to the cell surface expression and stabilization of the $Ca_v\alpha1$ pore channel unit, and thus controlling the extent of activation of the Ca++ influx in neurons as well as in cardiomyocytes. This is performed by promoting $Ca_v\alpha1$ translocation from the SR compartment, as well as stabilization of the $Ca_v\alpha1$ at the plasma membrane (Canti et al., 2005; Cassidy et al., 2014; Tran-Van-Minh and Dolphin, 2010). It is not clear however how protein translocation is promoted by $\alpha2\delta$. It is possible that SR to T-tubules juxtaposition enhances translocation of plasma membrane proteins from the SR to T-tubules in muscle fibers.

Larvae homozygous mutant for *Ma2/d* exhibited impaired locomotion. We cannot distinguish between the role of Ma2/d in regulating T-tubules-SR-nuclear contacts and its contribution to the stability of the plasma membrane $Ca_v\alpha1$ pore channel at the muscle side. We assume that both functions are necessary for proper larval locomotion. Importantly, both Msp300 and Amph mutant larvae exhibit similarly defective locomotion, implicating their contribution to proper muscle funationality.

In conclusion, our experiments uncover novel cellular and molecular aspects mediating membrane organelle connections in myofibers along the nuclei through the activity of *Ma2/d.* These contacts presumably contribute to an efficient transfer of mRNAs, proteins, and ions between organelles enabling proper muscle function.

Materials and Methods

Fly stocks

Fly stocks used in this study included w^{1118} (used as control wild type); P{GAL4-Mef2.R}; Df(2L)BSC293/CyO(YFP); Df(2L)msp300$^{\Delta 3'}$/CyO(YFP); *amph*^{2j6}; P{EPgy2}CG42817; P{TRIP.JF01922}attP2 (all of which were obtained from the Bloomington Drosophila Stock Center). *Ma2/d* mutants were obtained through imprecise excision of EPgy2^{EY09750} by standard procedure. The P-element excision produced rearrangement of the intronic sequences juxtapose to the end of the first exon (see supplementary Figure 2, according to Flybase (Gramates et al., 2017)). For the rescue experiments flies carrying either UAS- Ma2/d-GFP together Df(2L)BSC293/CyOYFP were

crossed to flies carrying excised EPgy2^{EY09750}/CyOYFP together with Mef2-GAL4/+. Mutants were identified by their negative YFP-deficient balancer.

Expression constructs

The full length CG42817 was amplified from cDNA clone RE14947 (GenBank accession number: BT021312, from Drosophila Genomics Resource Center), using the Gateway Cloning Technology (Invitrogen Life Technologies, USA). The gene was amplified using SuperTaq Plus polymerase enzyme (Invitrogen Life Technologies, USA), and inserted into the Gateway pDonor-201 vector using the following primers: attB1-FW Primer: 5'-GGGGACAAGTTTGTACAAAAAAGCAGGCTTCATGTTTGGTTTATGCGAAAAG-3', attB2-RV primer: 5'-GGG.GACCACTTTGTACAAGAAAGCTGGGTCACGCATAAAGCTGTGCGTCAG-3'. The insert was then transferred to two types of destination vectors: pTWG, which contains a 5'UAS promoter and 3' eGFP tag (used for transgenic flies). Full length Ma2/d-GFP was injected and transgenic flies obtained from BestGene company.

Immunochemical reagents

Primary antibody staining was performed overnight at 4^{o}C, and the secondary staining was performed for 2 h at room temperature. We used the following primary antibodies: guinea pig anti–MSP-300 (dilution 1:300) (Volk, 1992). Anti-Drosophila lamin C (dilution 1:10) LC28.26, anti-DLG 4F3 (dilution 1:50) were developed by Riemer et al (Riemer et al., 1995) and by Parnas et al., (Parnas et al., 2001) respectively, were obtained from the Developmental Studies Hybridoma Bank, created by the NICHD of the NIH and maintained at The University of Iowa, Department of Biology, Iowa City, IA 52242. Chick

anti-GFP (Abcam ab13970 dilution 1:200); rabbit anti-SERCA (obtained from Dr. Mani Ramaswami, Trinity College, Dublin, UK, dilution 1:200)(Sanyal et al., 2006); rabbit anti-Amphiphysin (obtained from Dr. Harvey T McMahon, MRC Laboratory of Molecular Biology, Cambridge UK, dilution 1:200)(Razzaq et al., 2001). Mouse anti-GFP (Roche) was used for Western blotting (dilution 1:1000). Rat anti- Ma2/d was raised against a mixture of 3 KLH-conjugated peptides from the Ma2/d sequence: peptide1- CKTYDPKTSNEKRPR, peptide2- CKSSASKPKDDSDDE, (both conjugated to a KLH N-terminus domain), and peptide3- KLNMSFYERRRIEEC (conjugated to a KLH C-terminus domain) (Peptide 2.0 Inc. Chantilly, VA. USA). The antibody was used at 1:500 for immunostaining, and at 1:1000 for Western blotting. Secondary antibodies conjugated with Cy3, Cy5, and Cy2 raised in either guinea pig, mouse, or rabbit were purchased from Jackson ImmunoResearch Laboratories (dilution 1:300). Alexa Fluor 488 (Thermo Fisher Scientific) was used at 1:200 and DAPI at 1:1000 dilution (Sigma).

Fixation and immunostaining

Staining of larval flat preparations:

Third instar larvae were selected and pinned on Sylgard plates (silicone elastomer-coated Petri plates, prepared by using a cocktail obtained from Dow Corning). The larvae were slit open, cleaned from fat bodies and organs, and fixed in 4% Paraformaldehyde (PFA) in Phoasohate Buffere Saline (PBS) for 25 min followed by blocking with 10% Bovine Serum Albumin (BSA) in PBS with 0.1% Triton X-100 (PBT) for 30 min The preparations were stained overnight with primary antibody in PBT, washed with PBT, reacted with secondary antibody for 1 h, washed with PBT, and mounted using Immu-

Mount solution (Thermo Fisher Scientific) on a glass slide such that the somatic muscles faced the coverslip.

Immaginal-Dics Staining

Third instar larvae expressing Ma2/d-GFP driven by the *P{GAL4}hhGal4* driver were dissected and the wing imanigal discs were fixed and stained with anti-GFP and anti Ma2/d.

mCLING labeling and immunostaining of Drosophila larval flat preparations.

The protocol was described by Revelo et., al., and used with minor modifications (Revelo and Rizzoli, 2016). The larvae were dissected using ice-cold physiological buffer without Ca2+, cleaned from fat bodies and organs, and incubated with mCLING probe (Synaptic Systems Cat. No. 710006AT1) at a concentration of 1.7 mM in physiological buffer without Ca2+ for 10 min at room temperature. The sample was then briefly wash with dye-free Ca2+-free solution and immediately fixed in 4%PFA+0.2% glutaraldehyde in PBS for 20 min on ice followed by 20 min incubation at room temp. The sample was then briefly washed with PBS and incubated for 5 min in quenching solution (Sodium Borohydride in 50ml PBS). The sample was then briefly washed in PBS and placed in antigen retrieval solution (RD Systems, USA) for 10 min at 95^{o}C followed by 10 min sample cooling at room temp, and an immediate 5 min wash in distilled water. The sample was then incubated in permeabilization solution, containing 0.5% Triton X-100 + 2.5% BSA in PBS, 3X10 min, and then incubated with the primary antibody, chicken anti-GFP at 1:50 (in 0.5% Triton X-100 + 2.5% BSA in PBS) for 1h at room temp. The sample was then washed 3X10 min in 0.5% Triton X-100 + 2.5% BSA in PBS, and incubated for 1h with secondary antibody, Goat anti-Chicken, Alexa Fluor

488, and 4',6-diamidino-2-phenylindole (DAPI). The sample was then washed 3X10 min in high-salt phosphate-buffer saline (PBS), pH 7.4 (500mM NaCl, 20mM Na_2HPO_4) followed by 2X10 min wash in PBS. Finally, the sample was mounded in 2,2′ -thiodiethanol (TDE) mounting medium (Abberior Cat. No. 4-0100-001-2) and immediately imaged under confocal microscope.

Western blotting and immunoprecipitation

Third instar larvae were collected and crushed in RIPA buffer (1% Triton X-100, 0.1% SDS, 0.15 M NaCl, and 0.05 Tris, pH 7, protease inhibitors mixture (P 8340; Sigma-Aldrich), then incubated on ice for 20 min

For immunoprecipitation, equal amounts of protein lysate were incubated overnight at 4°C with protein A/G beads (SC-2003, Santa Cruz Biotechnology, Inc.) or with GFP-TrapR_A beads (Chromotek, BioNovus Life Sciences) coupled with guinea pig anti–MSP-300 polyclonal antibody or rat anti Ma2/d antibody, respectively. Beads were washed three times with the RIPA lysis buffer and boiled in protein sample buffer to elute the proteins. Western analysis was performed according to standard procedures, as described previously (Volk, 1992).

Statistical Analysis

Distances between neighboring nuclei of muscle 6 were calculated using Fiji and the statistical program R, a language and environment for statistical computing. R Foundation for statistical computing, Austria (R core Team, 2016). URL https://www.R-project.org.

For statistics of nuclear associated SERCA - Data was acquired using a confocal microscope (Zeiss LSM 800) and analysis was performed using the profile tool (Zeiss, Zen). The average SERCA fluorescence intensity at the

nuclear periphery (labeled with anti Lamin C) relative to the nuclear interior along the nuclear meridian (Delta SERCA fluorescence) was measured. Similarly Lamin C levels at the nuclear periphery were measured. Numerical analysis and statistics were performed using Excel.

Microscopy and Image Analysis

Microscopic images were acquired at 23°C with confocal microscopes (LSM 800; Carl Zeiss) using ZEN 2.3 system software and the following lenses: Plan-Apochromat 20×/0.8 NA M27, C-Apochromat 40×/1.20 NA W Korr M27, and Plan-Apochromat 63×/1.40 NA oil differential interference contrast (DIC) M27. Immersion medium Immersol W 2010 (ne = 1.3339) and Immersion oil Immersol 518 F (ne = 1.518) were used, respectively.

Movies of intact larvae

To visualize muscle dynamics of the muscle, we used a chamber developed by Ghannad-Rezaie (Ghannad-Rezaie et al., 2012). A third instar larvae expressing Ma2/d-GFP driven by Mef-GAL4, was positioned in the chamber, immobilized, and placed on the stage of a VisiScope CSU-W1 Spinning Disk Confocal Microscope (Visitron Systems GmbH) attached to an Olympus IX83 inverted microscope. The images were acquired with a 60X oil immersion objective, and the acquisition duration of each image was 50 msec.

Locomotion analysis was performed essentially as described in Elhanany-Tamir et al (Elhanany-Tamir et al., 2012).

Acknowledgement

We thank the Bloomington Stock Centre for various fly lines, the Developmental Studies Hybridoma Bank (DSHB) for antibodies, and FlyBase for important genomic information. We are grateful to Mani Ramaswami, and Harvey McMahon, for providing valuable primary antibodies. This study was supported by a grant from the MINERVA foundation 711743 (TV). FlyBase is supported by a grant from the National Human Genome Research Institute at the U.S. National Institutes of Health #U41 HG000739. Support is also provided by the British Medical Research Council (#MR/N030117/1) and the Indiana Genomics Initiative. The BDSC is supported by a grant from the Office of the Director of the National Institues of Health under Award Number P40OD018537. NIH ICs OD, NIGMS, NICHD and NINDS contribute to funding of this award.

References

Adam, J., N. Basnet, and N. Mizuno. 2015. Structural insights into the cooperative remodeling of membranes by amphiphysin/BIN1. *Sci Rep*. 5:15452.

Bank, E.M., K. Ben-Harush, N. Wiesel-Motiuk, R. Barkan, N. Feinstein, O. Lotan, O. Medalia, and Y. Gruenbaum. 2011. A laminopathic mutation disrupting lamin filament assembly causes disease-like phenotypes in Caenorhabditis elegans. *Mol Biol Cell*. 22:2716-2728.

Block, B.A., T. Imagawa, K.P. Campbell, and C. Franzini-Armstrong. 1988. Structural evidence for direct interaction between the molecular components of the transverse tubule/sarcoplasmic reticulum junction in skeletal muscle. *J. Cell Biol.* 107:2587-2600.

Cadot, B., V. Gache, and E.R. Gomes. 2015. Moving and positioning the nucleus in skeletal muscle - one step at a time. *Nucleus*. 6:373-381.

Cain, N.E., E.C. Tapley, K.L. McDonald, B.M. Cain, and D.A. Starr. 2014. The SUN protein UNC-84 is required only in force-bearing cells to maintain nuclear envelope architecture. *J. Cell Biol.* 206:163-172.

Caldwell, J.L., C.E. Smith, R.F. Taylor, A. Kitmitto, D.A. Eisner, K.M. Dibb, and A.W. Trafford. 2014. Dependence of cardiac transverse tubules on the BAR domain protein amphiphysin II (BIN-1). *Circ Res*. 115:986-996.

Canti, C., M. Nieto-Rostro, I. Foucault, F. Heblich, J. Wratten, M.W. Richards, J. Hendrich, L. Douglas, K.M. Page, A. Davies, and A.C. Dolphin. 2005. The metal-ion-dependent adhesion site in the Von Willebrand factor-A domain of alpha2delta subunits is key to trafficking voltage-gated Ca2+ channels. *Proc Natl Acad Sci U S A*. 102:11230-11235.

Cassidy, J.S., L. Ferron, I. Kadurin, W.S. Pratt, and A.C. Dolphin. 2014. Functional exofacially tagged N-type calcium channels elucidate the interaction with auxiliary alpha2delta-1 subunits. *Proc Natl Acad Sci U S A*. 111:8979-8984.

Clark, K.A., A.S. McElhinny, M.C. Beckerle, and C.C. Gregorio. 2002. Striated muscle cytoarchitecture: an intricate web of form and function. *Annu. Rev. Cell. Dev. Biol.* 18:637-706.

D'Alessandro, M., K. Hnia, V. Gache, C. Koch, C. Gavriilidis, D. Rodriguez, A.S. Nicot, N.B. Romero, Y. Schwab, E. Gomes, M. Labouesse, and J. Laporte. 2015. Amphiphysin 2 Orchestrates Nucleus Positioning and Shape by Linking the Nuclear Envelope to the Actin and Microtubule Cytoskeleton. *Dev. Cell*. 35:186-198.

D'Arco, M., W. Margas, J.S. Cassidy, and A.C. Dolphin. 2015. The upregulation of alpha2delta-1 subunit modulates activity-dependent Ca2+ signals in sensory neurons. *J. Neurosci.* 35:5891-5903.

Dialynas, G., K.M. Flannery, L.N. Zirbel, P.L. Nagy, K.D. Mathews, S.A. Moore, and L.L. Wallrath. 2012. LMNA variants cause cytoplasmic distribution of nuclear pore proteins in Drosophila and human muscle. *Hum. Mol. Genet.* 21:1544-1556.

Dialynas, G., S. Speese, V. Budnik, P.K. Geyer, and L.L. Wallrath. 2010. The role of Drosophila Lamin C in muscle function and gene expression. *Development*. 137:3067-3077.

Dolphin, A.C. 2012. Calcium channel auxiliary alpha2delta and beta subunits: trafficking and one step beyond. *Nat. Rev. Neurosci.* 13:542-555.

Dolphin, A.C. 2013. The alpha2delta subunits of voltage-gated calcium channels. *Biochim. Biophys. Acta*. 1828:1541-1549.

Elhanany-Tamir, H., Y.V. Yu, M. Shnayder, A. Jain, M. Welte, and T. Volk. 2012. Organelle positioning in muscles requires cooperation between two KASH proteins and microtubules. *J. Cell Biol.* 198:833-846.

Eroglu, C., N.J. Allen, M.W. Susman, N.A. O'Rourke, C.Y. Park, E. Ozkan, C. Chakraborty, S.B. Mulinyawe, D.S. Annis, A.D. Huberman, E.M. Green, J. Lawler, R. Dolmetsch, K.C. Garcia, S.J. Smith, Z.D. Luo, A. Rosenthal, D.F. Mosher, and B.A. Barres. 2009. Gabapentin receptor alpha2delta-1 is a neuronal thrombospondin receptor responsible for excitatory CNS synaptogenesis. *Cell*. 139:380-392.

Falcone, S., W. Roman, K. Hnia, V. Gache, N. Didier, J. Laine, F. Aurade, I. Marty, I. Nishino, N. Charlet-Berguerand, N.B. Romero, G. Marazzi, D. Sassoon, J. Laporte, and E.R. Gomes. 2014. N-WASP is required for Amphiphysin-2/BIN1-dependent nuclear positioning and triad organization in skeletal muscle and is involved in the pathophysiology of centronuclear myopathy. *EMBO Mol Med*. 6:1455-1475.

Fischer, J.A., S. Acosta, A. Kenny, C. Cater, C. Robinson, and J. Hook. 2004. Drosophila klarsicht has distinct subcellular localization domains for nuclear envelope and microtubule localization in the eye. *Genetics*. 168:1385-1393.

Folker, E.S., and M.K. Baylies. 2013. Nuclear positioning in muscle development and disease. *Front Physiol*. 4:363.

Folker, E.S., V.K. Schulman, and M.K. Baylies. 2012. Muscle length and myonuclear position are independently regulated by distinct Dynein pathways. *Development*. 139:3827-3837.

Folker, E.S., V.K. Schulman, and M.K. Baylies. 2014. Translocating myonuclei have distinct leading and lagging edges that require kinesin and dynein. *Development*. 141:355-366.

Garcia, K., T. Nabhani, and J. Garcia. 2008. The calcium channel alpha2/delta1 subunit is involved in extracellular signalling. *J Physiol*. 586:727-738.

Gautel, M., and K. Djinovic-Carugo. 2016. The sarcomeric cytoskeleton: from molecules to motion. *J. Exp. Biol.* 219:135-145.

Ghannad-Rezaie, M., X. Wang, B. Mishra, C. Collins, and N. Chronis. 2012. Microfluidic chips for in vivo imaging of cellular responses to neural injury in Drosophila larvae. *PloS one*. 7:e29869.

Gramates, L.S., S.J. Marygold, G.D. Santos, J.M. Urbano, G. Antonazzo, B.B. Matthews, A.J. Rey, C.J. Tabone, M.A. Crosby, D.B. Emmert, K. Falls, J.L. Goodman, Y. Hu, L. Ponting, A.J. Schroeder, V.B. Strelets, J. Thurmond, P. Zhou, and C. the FlyBase. 2017. FlyBase at 25: looking to the future. *Nucleic Acids Res.* 45:D663-D671.

Gundersen, G.G., and H.J. Worman. 2013. Nuclear positioning. *Cell*. 152:1376-1389.

Hong, T., and R.M. Shaw. 2017. Cardiac T-Tubule Microanatomy and Function. *Physiol. Rev.* 97:227-252.

Jungbluth, H., and M. Gautel. 2014. Pathogenic mechanisms in centronuclear myopathies. *Front Aging Neurosci*. 6:339.

Kracklauer, M.P., S.M. Banks, X. Xie, Y. Wu, and J.A. Fischer. 2007. Drosophila klaroid encodes a SUN domain protein required for Klarsicht localization to the nuclear envelope and nuclear migration in the eye. *Fly (Austin)*. 1:75-85.

Lee, E., M. Marcucci, L. Daniell, M. Pypaert, O.A. Weisz, G.C. Ochoa, K. Farsad, M.R. Wenk, and P. De Camilli. 2002. Amphiphysin 2 (Bin1) and T-tubule biogenesis in muscle. *Science*. 297:1193-1196.

Ly, C.V., C.K. Yao, P. Verstreken, T. Ohyama, and H.J. Bellen. 2008. straightjacket is required for the synaptic stabilization of cacophony, a voltage-gated calcium channel alpha1 subunit. *J. Cell Biol.* 181:157-170.

Mathew, D., A. Popescu, and V. Budnik. 2003. Drosophila amphiphysin functions during synaptic Fasciclin II membrane cycling. *J. Neurosci.* 23:10710-10716.

Mattout, A., B.L. Pike, B.D. Towbin, E.M. Bank, A. Gonzalez-Sandoval, M.B. Stadler, P. Meister, Y. Gruenbaum, and S.M. Gasser. 2011. An EDMD mutation in C. elegans lamin blocks muscle-specific gene relocation and compromises muscle integrity. *Curr. Biol.* 21:1603-1614.

McGee, M.D., R. Rillo, A.S. Anderson, and D.A. Starr. 2006. UNC-83 IS a KASH protein required for nuclear migration and is recruited to the outer nuclear membrane by a physical interaction with the SUN protein UNC-84. *Mol Biol Cell*. 17:1790-1801.

Metzger, T., V. Gache, M. Xu, B. Cadot, E.S. Folker, B.E. Richardson, E.R. Gomes, and M.K. Baylies. 2012. MAP and kinesin-dependent nuclear positioning is required for skeletal muscle function. *Nature*. 484:120-124.

Mim, C., and V.M. Unger. 2012. Membrane curvature and its generation by BAR proteins. *Trends Biochem. Sci.* 37:526-533.

Morel, V., S. Lepicard, A.N. Rey, M.L. Parmentier, and L. Schaeffer. 2014. Drosophila Nesprin-1 controls glutamate receptor density at neuromuscular junctions. *Cell. Mol. Life Sci.* 71:3363-3379.

Muchir, A., and H.J. Worman. 2007. Emery-Dreifuss muscular dystrophy. *Curr Neurol Neurosci Rep*. 7:78-83.

Neely, G.G., A. Hess, M. Costigan, A.C. Keene, S. Goulas, M. Langeslag, R.S. Griffin, I. Belfer, F. Dai, S.B. Smith, L. Diatchenko, V. Gupta, C.P. Xia, S. Amann, S. Kreitz, C. Heindl-Erdmann, S. Wolz, C.V. Ly, S. Arora, R. Sarangi, D. Dan, M. Novatchkova, M. Rosenzweig, D.G. Gibson, D. Truong, D. Schramek, T. Zoranovic, S.J. Cronin, B. Angjeli, K. Brune, G. Dietzl, W. Maixner, A. Meixner, W. Thomas, J.A. Pospisilik, M. Alenius, M. Kress, S. Subramaniam, P.A. Garrity, H.J. Bellen, C.J. Woolf, and J.M. Penninger. 2010. A genome-wide Drosophila screen for heat nociception identifies alpha2delta3 as an evolutionarily conserved pain gene. *Cell*. 143:628-638.

Packard, M., V. Jokhi, B. Ding, C. Ruiz-Canada, J. Ashley, and V. Budnik. 2015. Nucleus to Synapse Nesprin1 Railroad Tracks Direct Synapse Maturation through RNA Localization. *Neuron*. 86:1015-1028.

Parnas, D., A.P. Haghighi, R.D. Fetter, S.W. Kim, and C.S. Goodman. 2001. Regulation of postsynaptic structure and protein localization by the Rho-type guanine nucleotide exchange factor dPix. *Neuron*. 32:415-424.

Puckelwartz, M., and E.M. McNally. 2011. Emery-Dreifuss muscular dystrophy. *Handb Clin Neurol*. 101:155-166.

Puckelwartz, M.J., E. Kessler, Y. Zhang, D. Hodzic, K.N. Randles, G. Morris, J.U. Earley, M. Hadhazy, J.M. Holaska, S.K. Mewborn, P. Pytel, and E.M. McNally. 2009. Disruption of nesprin-1 produces an Emery Dreifuss muscular dystrophy-like phenotype in mice. *Hum. Mol. Genet.* 18:607-620.

Razzaq, A., I.M. Robinson, H.T. McMahon, J.N. Skepper, Y. Su, A.C. Zelhof, A.P. Jackson, N.J. Gay, and C.J. O'Kane. 2001. Amphiphysin is necessary for organization of the excitation-contraction coupling machinery of muscles, but not for synaptic vesicle endocytosis in Drosophila. *Genes Dev.* 15:2967-2979.

Revelo, N.H., and S.O. Rizzoli. 2016. The Membrane Marker mCLING Reveals the Molecular Composition of Trafficking Organelles. *Curr Protoc Neurosci*. 74:2 25 21-21.
Ribeiro, I., L. Yuan, G. Tanentzapf, J.J. Dowling, and A. Kiger. 2011. Phosphoinositide regulation of integrin trafficking required for muscle attachment and maintenance. *PLoS Genet.* 7:e1001295.
Riemer, D., N. Stuurman, M. Berrios, C. Hunter, P.A. Fisher, and K. Weber. 1995. Expression of Drosophila lamin C is developmentally regulated: analogies with vertebrate A-type lamins. *J. Cell Sci.* 108 (Pt 10):3189-3198.
Royer, B., K. Hnia, C. Gavriilidis, H. Tronchere, V. Tosch, and J. Laporte. 2013. The myotubularin-amphiphysin 2 complex in membrane tubulation and centronuclear myopathies. *EMBO Rep*. 14:907-915.
Sanyal, S., T. Jennings, H. Dowse, and M. Ramaswami. 2006. Conditional mutations in SERCA, the Sarco-endoplasmic reticulum Ca2+-ATPase, alter heart rate and rhythmicity in Drosophila. *J Comp Physiol B*. 176:253-263.
Schulman, V.K., E.S. Folker, J.N. Rosen, and M.K. Baylies. 2014. Syd/JIP3 and JNK signaling are required for myonuclear positioning and muscle function. *PLoS Genet.* 10:e1004880.
Starr, D.A., and M. Han. 2002. Role of ANC-1 in tethering nuclei to the actin cytoskeleton. *Science*. 298:406-409.
Subramanian, A., and T.F. Schilling. 2014. Thrombospondin-4 controls matrix assembly during development and repair of myotendinous junctions. *eLife*. 3.
Subramanian, A., B. Wayburn, T. Bunch, and T. Volk. 2007. Thrombospondin-mediated adhesion is essential for the formation of the myotendinous junction in Drosophila. *Development*. 134:1269-1278.
Technau, M., and S. Roth. 2008. The Drosophila KASH domain proteins Msp-300 and Klarsicht and the SUN domain protein Klaroid have no essential function during oogenesis. *Fly (Austin)*. 2:82-91.
Tian, X., U. Gala, Y. Zhang, W. Shang, S. Nagarkar Jaiswal, A. di Ronza, M. Jaiswal, S. Yamamoto, H. Sandoval, L. Duraine, M. Sardiello, R.V. Sillitoe, K. Venkatachalam, H. Fan, H.J. Bellen, and C. Tong. 2015. A voltage-gated calcium channel regulates lysosomal fusion with endosomes and autophagosomes and is required for neuronal homeostasis. *PLoS Biol.* 13:e1002103.
Tran-Van-Minh, A., and A.C. Dolphin. 2010. The alpha2delta ligand gabapentin inhibits the Rab11-dependent recycling of the calcium channel subunit alpha2delta-2. *J. Neurosci.* 30:12856-12867.
Volk, T. 1992. A new member of the spectrin superfamily may participate in the formation of embryonic muscle attachments in Drosophila. *Development*. 116:721-730.
Volk, T. 2012. Positioning nuclei within the cytoplasm of striated muscle fiber: Cooperation between microtubules and KASH proteins. *Nucleus*. 4.
Wang, S., A. Reuveny, and T. Volk. 2015. Nesprin provides elastic properties to muscle nuclei by cooperating with spectraplakin and EB1. *J. Cell Biol.* 209:529-538.
Yu, X., J. Ma, F. Lin, W. Zhao, X. Fu, and Z.J. Zhao. 2012. Myotubularin family phosphatase ceMTM3 is required for muscle maintenance by preventing excessive autophagy in Caenorhabditis elegans. *BMC Cell Biol.* 13:28.
Zhang, Q., C. Bethmann, N.F. Worth, J.D. Davies, C. Wasner, A. Feuer, C.D. Ragnauth, Q. Yi, J.A. Mellad, D.T. Warren, M.A. Wheeler, J.A. Ellis, J.N.

Skepper, M. Vorgerd, B. Schlotter-Weigel, P.L. Weissberg, R.G. Roberts, M. Wehnert, and C.M. Shanahan. 2007. Nesprin-1 and -2 are involved in the pathogenesis of Emery Dreifuss muscular dystrophy and are critical for nuclear envelope integrity. *Hum. Mol. Genet.* 16:2816-2833.

Figures

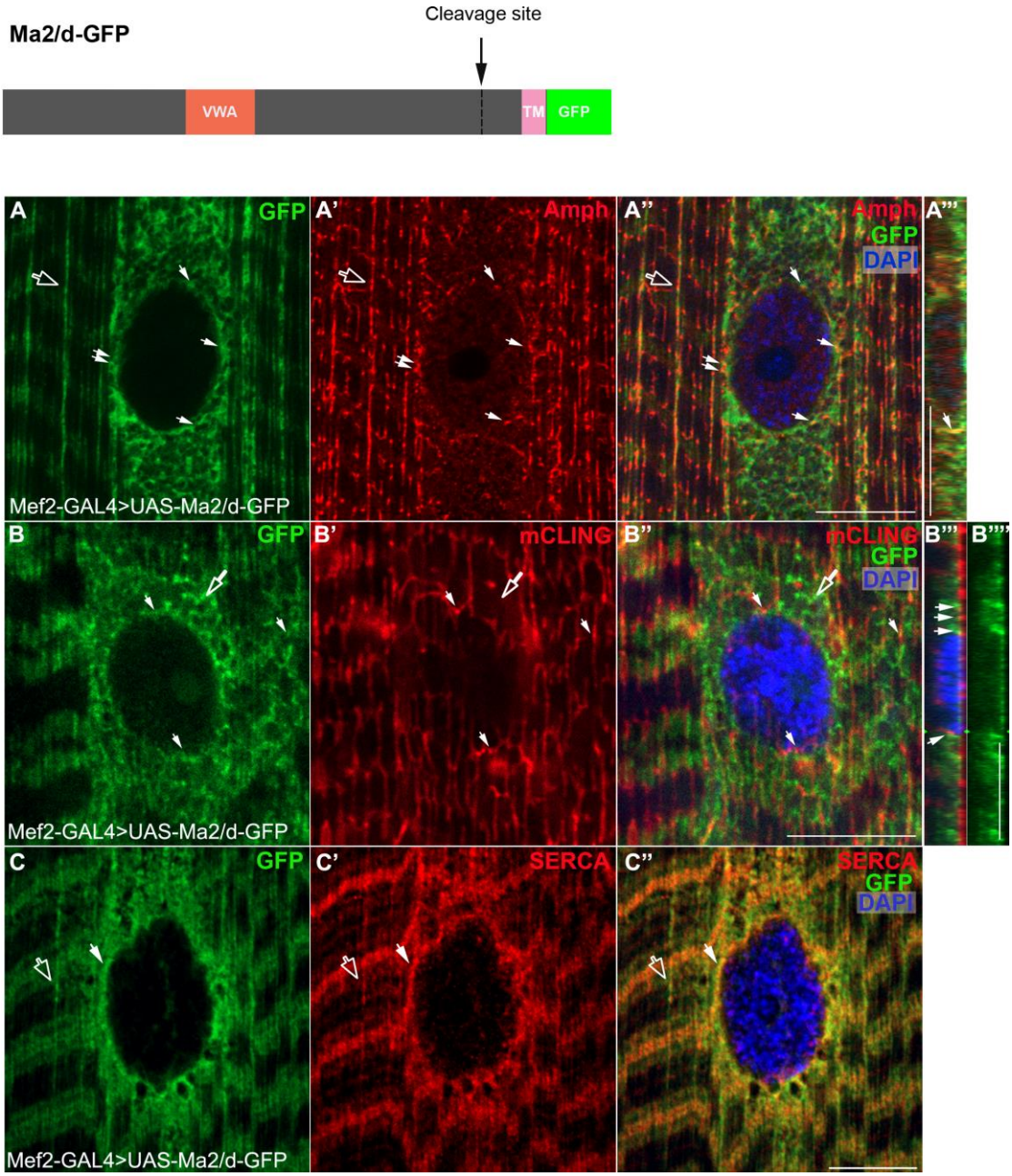

Figure 1: Ma2/delta-GFP localization in myofibers corresponds to SR and T-tubules

Upper panel: domain structure of Ma2/d-GFP.

(A-C) Single confocal images of flat preps of 3rd instar larval muscles expressing Ma2/d-GFP (A-A’’’, B-B’’’’, C-C’’) and labeled with anti GFP (green, A,A’’,A’’’,B,B’’,B’’’,B’’’’, C,C’’) and with either anti Amphiphysin (red, A’,A’’,A’’’), mCLING (red, B’,B’’,B’’’), or anti SERCA (red, C’,C’’). A’’’, B’’’ and B’’’’ are orthogonal sections of the nuclei shown in A’’ or B’’ respectively. White filled arrows in A-A’’’ indicate sites along the myonuclei where Ma2/d-GFP and Amphiphysin co-localize. Empty arrows in A-A’’’ indicate longitudinal T-tubules. White arrows in B-B’’’’ indicate sites where Mα2d-GFP and mCLING are proximal. Empty arrows in B-B’’ indicate sites of negative overlap. White filled arrows in C-C’’ indicate sites of co-localization of Ma2/d-GFP and SERCA at the nuclear-associated SR, and empty arrows indicate sites of co-localization of Ma2/d-GFP and SERCA at the T-tubules. A-C panels show a single optical confocal stack. Bars in all panels indicate 10 μm.

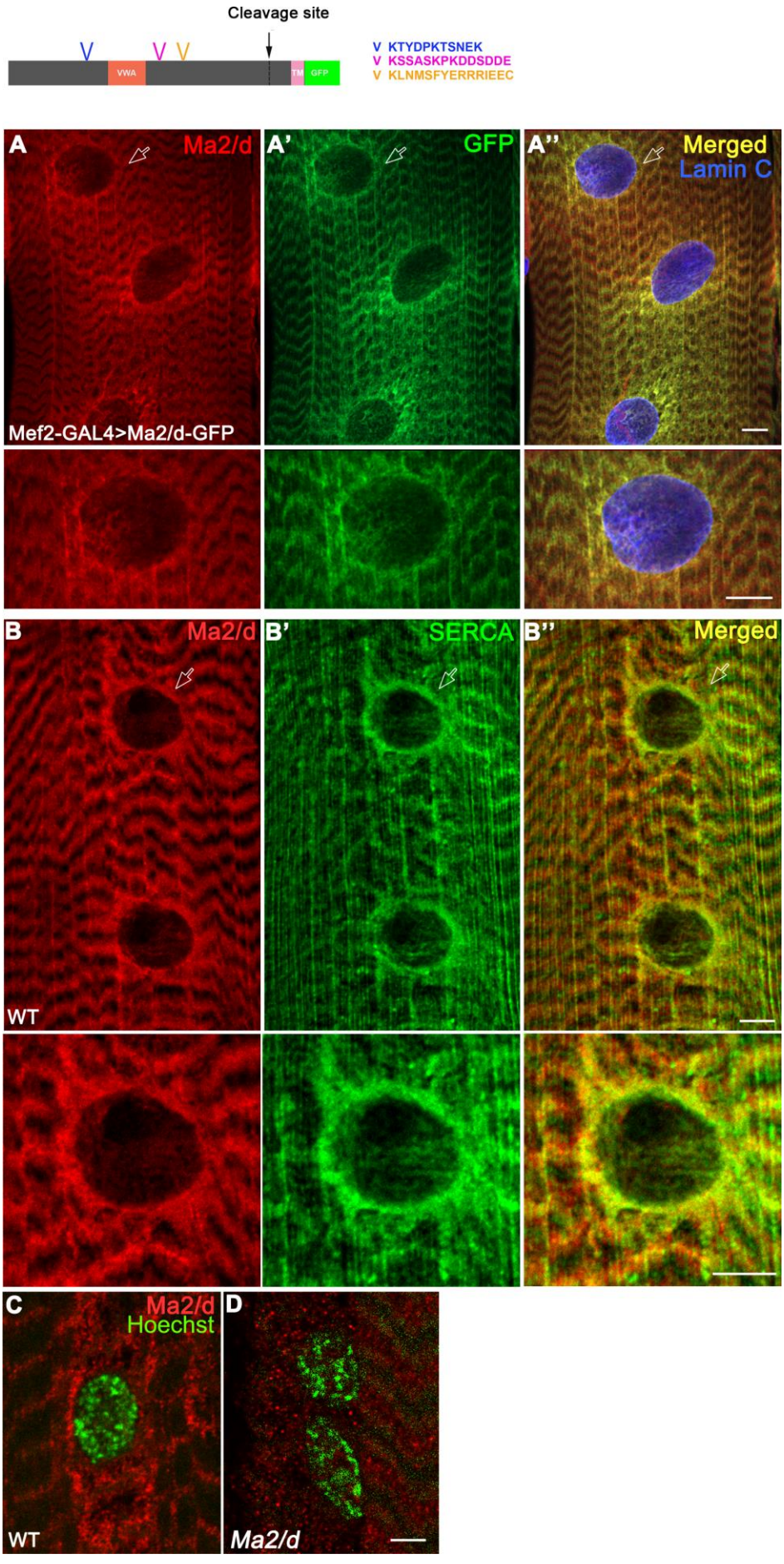

Figure 2: Ma2/d antibody reactivity in wild type and *Ma2/d* mutant muscles

Upper panel – three peptides used for production of the anti Ma2/d protein.

A-A'' – Single confocal stacks of larval muscles expressing Ma2/d-GFP labeled with anti Ma2/d antibody (A, red) and anti GFP (A', green). The nuclei are labeled with Lamin C (A'', blue). Enlarged images of single nuclei (marked by arrow) are shown in the lower panels indicating high degree of overlap between the anti Ma2/d and Ma2/d-GFP. B-B'' – single confocal stack of larval muscle labeled with anti Ma2/d, red), anti SERCA (green), and their merged image (B''). The nucleus indicated by an arrow is enlarged in the corresponding lower panels. Note an intense labeling for Ma2/d at the perinuclear region, which overlap with SERCA.

C,D – 3rd instar larval muscles stained with anti Ma2/d (red) in wild type (C), or in *Ma2/d* mutant (D) muscles. The antibody does not react with muscles of the mutant larvae. Hoechst labels the muscle nuclei (green). Bars in all panels indicate 10μm.

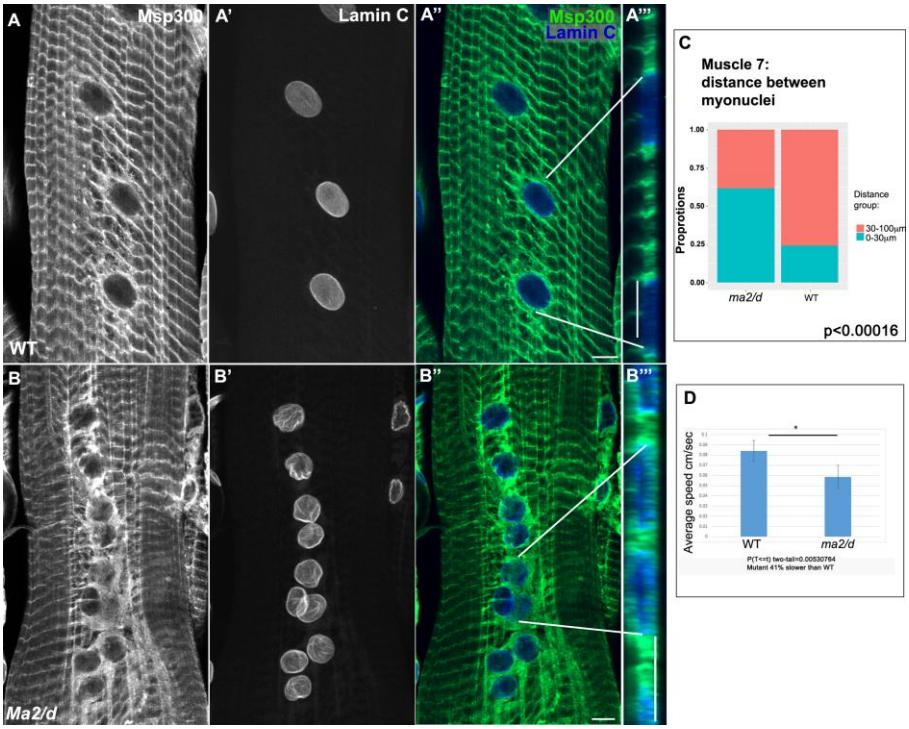

Figure 3: Ma2/d is required for nuclear positioning and proper Msp300 nuclear localization

Single confocal stacks of muscles from wild type (A-A''') and *Ma2/d* mutant (B-B''') labeled with anti Msp300 (green A'', A''', B'', B''') and anti lamin C (white A, A', B, B' and blue A'', A''', B'', B'''). Note the aberrant nuclear position in *Ma2/d* mutant muscles, and Msp300 accumulation around the nuclei. Orthogonal sections (A''', B''') indicate the accumulation of Msp300 above and around the myonuclei in mutant muscles. C- Quantification of the distances between nuclei of muscle 6 in WT and *Ma2/d* mutant. In the WT muscle, most of the nuclei were at a comparable distance of 30-200µm from each other (76.4%), whereas in *Ma2/d* mutant muscle most of the nuclei were closer to each other and only 37.4% were at a distance similar to wild type ($p<0.00016$). D – Quantification of the locomotion of WT and *Ma2/d* mutant larvae. N=7. $P<0.005$.

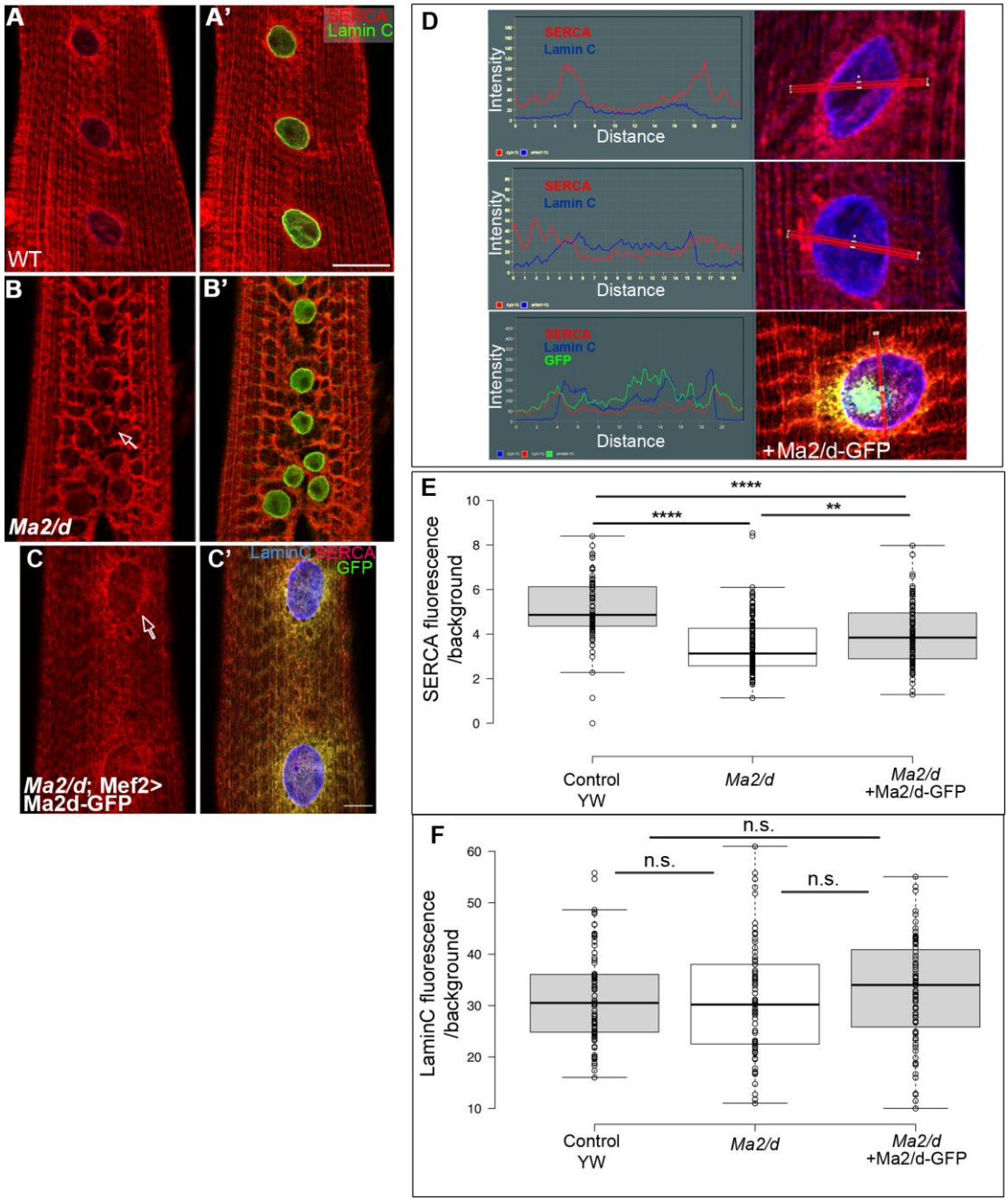

Figure 4: Decreased distribution of perinuclear SERCA in *Ma2/d* mutant muscles

Single confocal stacks of wild type (A,A') or *Ma/d* mutant (B,B') muscles labeled with anti SERCA (red, A-B') and anti Lamin C (green, A', B') are shown. Note that SERCA distribution is abnormal in the mutant and it is often

reduced at the nuclear membrane (arrow in B). D, E – Quantification of SERCA at the perinuclear region. D (upper and middle panels): Representative examples of the quantification method in which the fluorescent profile is taken from SERCA (red) or from Lamin C (blue) in wild type or *Ma2/d* mutant. The red box indicates the meridian axis. E - Quantification of peak SERCA fluorescence intensity/background (SERCA at the nuclear envelope normalized to SERCA in the center of the nucleus) along the nuclear meridian in control (YW) versus *Ma2/d* mutant muscles indicating a significant difference between the two groups (*t* test: p=9E-18; for WT n = 40 nuclei from 10 different muscles from 3 distinct larvae were quantified. For *Ma2/d* n = 29 nuclei from 8 different muscles from 3 distinct larvae were quantified). C, C' – representative image of rescue experiment demonstrating single confocal stacks of larval muscle in which Ma2/d-GFP driven by the Mef2-GAL4 driver was expressed in a *Ma2/d* mutant larva (red, SERCA), C' - merged images of SERCA (red), Ma2/d-GFP (green) and Lam C (blue). D – (lowest panel) shows example of the fluorescent profile of the rescue experiment. Quantification of SERCA levels in the rescue experiment is shown in E, relative to *Ma2/d* mutant and relative to control.

A significant difference between the rescue and the mutant groups is observed (*t* test p=0.001; The rescue group included n=37 nuclei, analyzed from 10 muscles from 5 distinct larvae). SERCA levels in the rescue group did not reach the levels of control and there was a significant difference between the groups (*t* test p=2.9E-10), implying only partial rescue. F - Quantification of the corresponding Lamin C peak fluorescent/background (measured at the same focal plane as SERCA), in each of the experimental groups. No

significant difference between Lamin C levels in the control (YW) versus *Ma2/d* mutant muscles was observed (*t* test p= 0.3). No significant difference between Lamin C levels in the rescue group versus the control were observed (*t* test p= 0.2). No significant difference between the rescue group and the mutant group (*t* test p=0.1). Numbers of nuclei are the same as for SERCA. Bars in all panels indicate indicates 10μm.

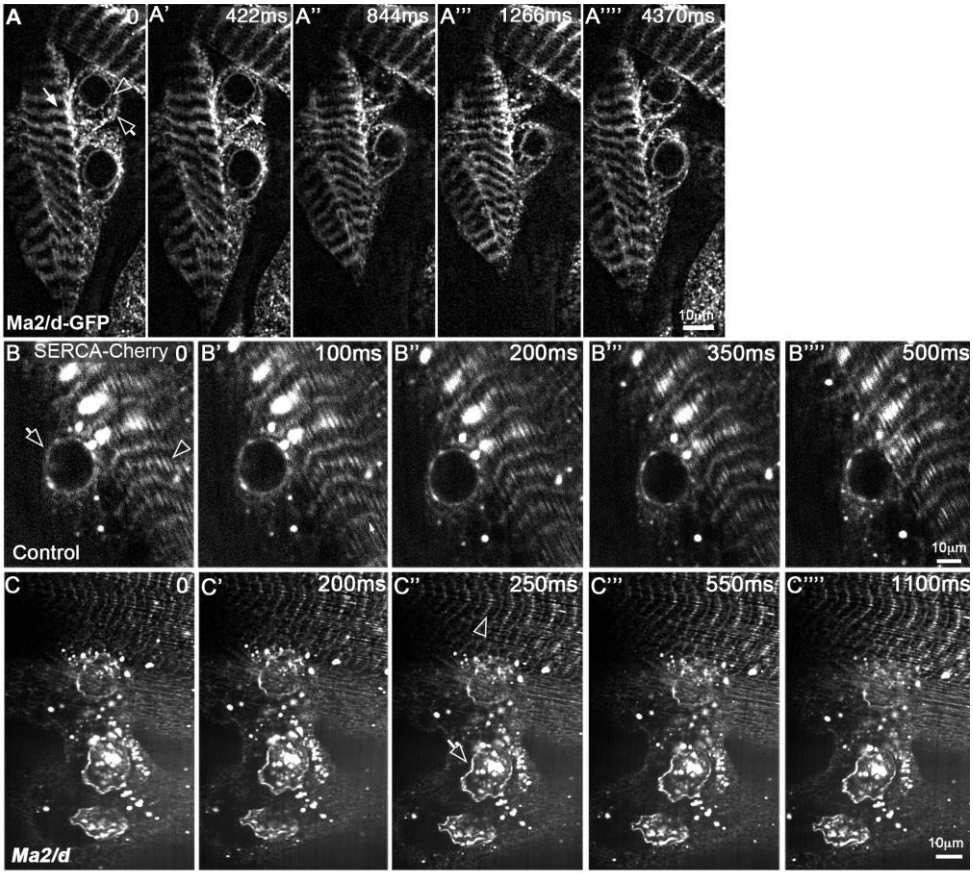

Figure 5: Live imaging of Ma2/d-GFP and SERCA-Cherry in control and *Ma2/d* mutant larval muscles

Steel images from a movie of live intact larvae expressing Ma2/d-GFP in muscles during a single contractile event. A-A'''' are images of distinct time series; ms – miliseconds. (The entire movie is shown in Supp material movie 1). Empty arrowhead and empty arrow in A indicate SR, filled arrow in A indicates T-tubules. Thin GFP-positive connectors are observed between the ER and the SR surrounding the nuclei (white arrow in A'). In the course of contraction (panels A'', A''') the Ma/d-GFP positive connections are still observed. B, C – Steel images from a movie of live intact larvae expressing SERCA-Cherry during contraction of wild type (B-B'''') or *Ma2/d* mutant (C-C'''') larvae. Arrows in B and C'' show SERCA around the nucleus and arrowheads in B and C'' show SERCA along the T-tubules.

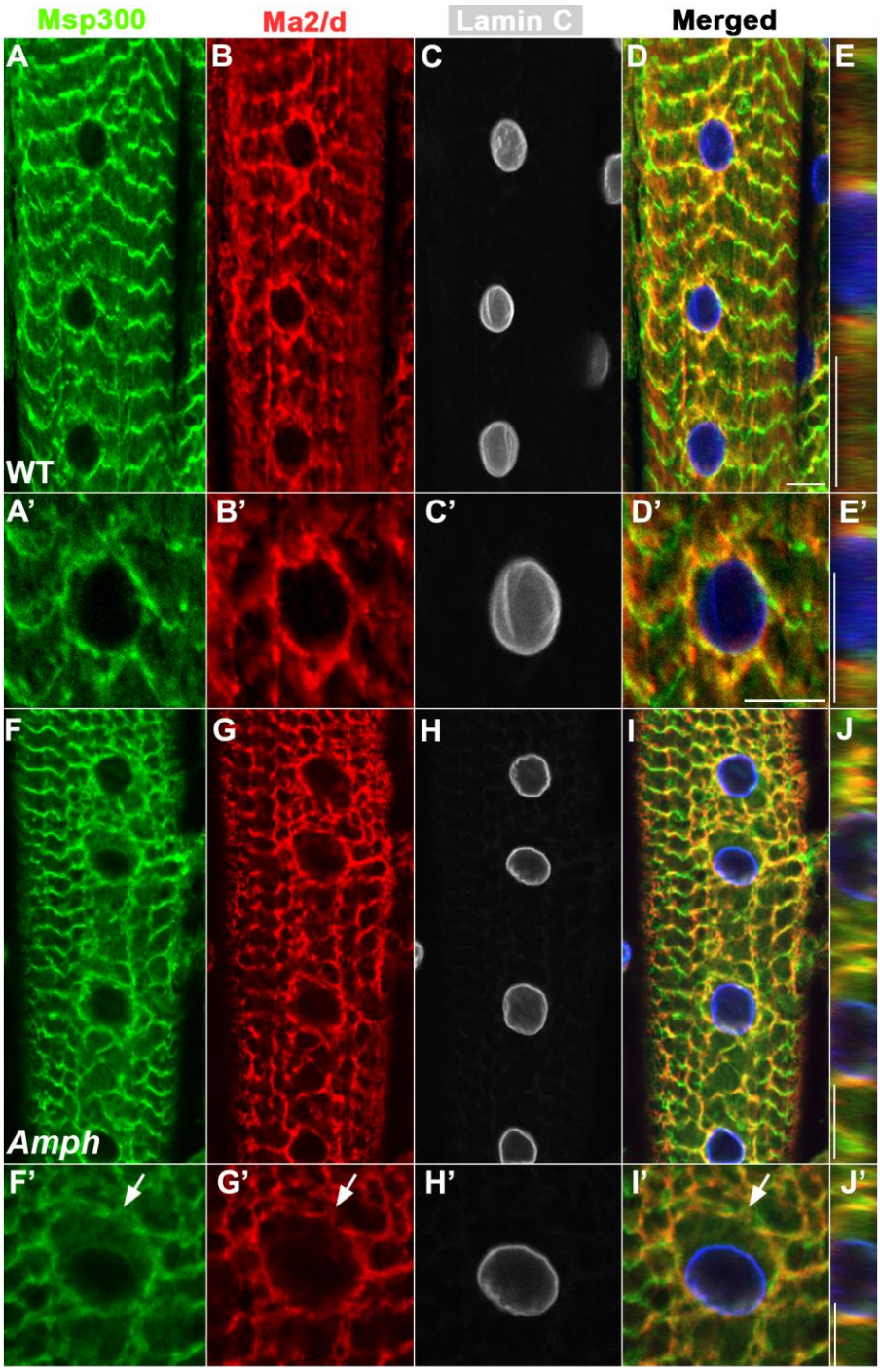

Figure 6: Ma2/d and Msp300 distribution along the SR depends on Amphiphysin

Muscles of wild type (A-E') and *Amph* mutant (F-J') of 3rd instar larvae, labeled with anti Msp300 (green, A,A',D,D', ,E, E', F, F', I, I',J, I',J'), anti Ma2/d (red,

B,B’,D,D’,E,E’,G,G’,I,I’, J,J’) and anti lamin C (white, C,C’,H,H’ and blue, D,D’,E,E’,I,I’,J,J’). A’-E’ and F’-J’ demonstrate corresponding enlarged images of single nuclei. In *Amph* mutant 42.9% of the myonuclei showed partial or complete dissociation of Ma2/d and Msp300 from the perinuclear distribution (n=46) mutant nuclei. In control 100% of the myonuclei showed normal perinuclear distribution of Ma2/d (n=76) or Msp300 (n=65). Arrows in F’, G’, I’ indicate sites where Msp300 and Ma2/d dissociate from the myonuclei.

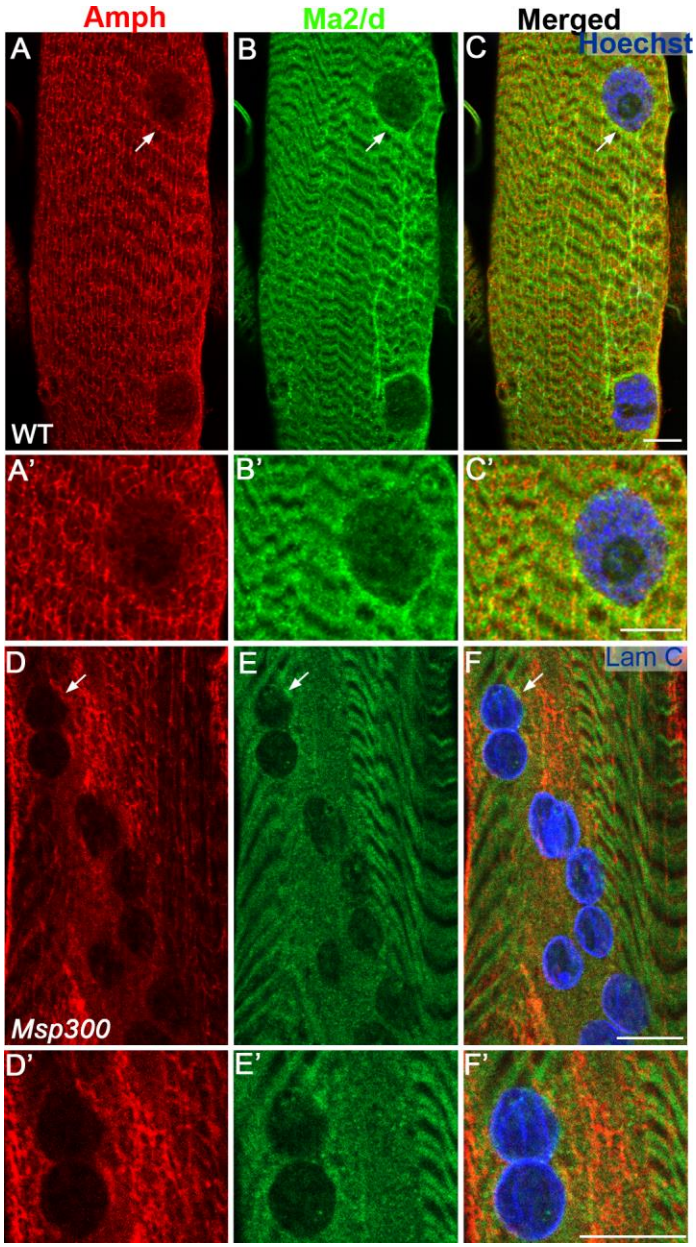

Figure 7: Amph and Ma2/d distributions at the nuclear periphery are disrupted in *Msp300* mutant muscles

Single representative confocal stacks of larval muscles from wild type (YW, A-C'), or *Msp300*$^{\Delta 3}$ mutant (D-F') labeled with Amph (red, A,A', D,D') and Ma2/d (green, B,B', E,E') and their merged panels (C,C', F,F') are shown. For *Msp300* mutants 98% of the nuclei showed complete loss of Amph and 99.6% of the nuclei showed complete or partial loss of Ma2/d (n = 118 nuclei). For

wild type 100% of the nuclei showed normal perinuclear distribution for Amph (n=93), and for Ma2/d (n=76). The nuclei indicated by white arrows (A-C and D-F) are shown in higher magnification in the corresponding panels (A'-C' and D'-F'). Bar indicates 10μm.

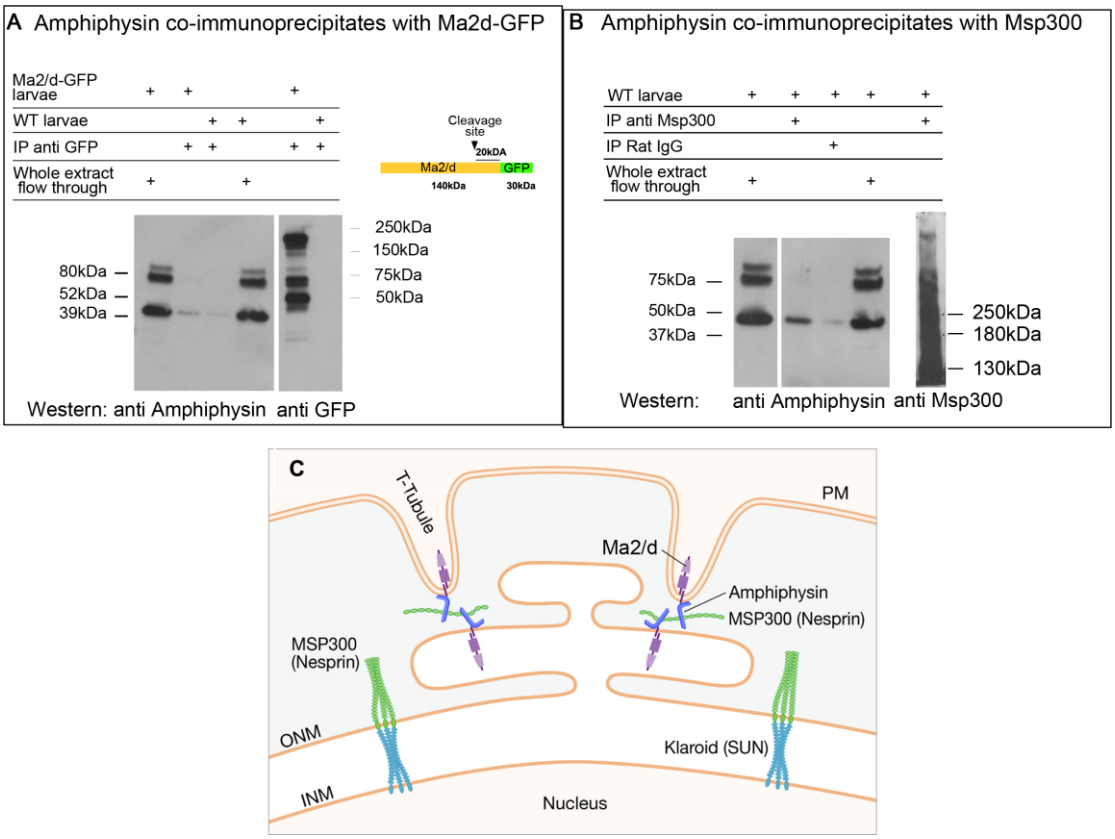

Figure 8: Amph co-precipitates with Ma2/d and with Msp300

A – Left panel: Immunoprecipitation of Ma2/d-GFP expressed in larval muscles using anti GFP antibody followed by western analysis with anti Amph indicates a band corresponding to Amph lower band (~39kDa), which is stronger relative to control. Whole extract flow-through of the anti GFP beads indicates equal loading. Right panel: GFP IP from control (WT) and larvae expressing Ma2/d-GFP reacted with anti GFP, indicates the 170kDa intact Ma2/d-GFP, as well as the 120kDa and 50kDa cleaved forms of Ma2/d-GFP.

B – Left and middle panels: Immunoprecipitation with anti Msp300 antibody followed by Western with anti Amph indicates a lower Amph specific band (~39kDa) which is stronger relative to control. Whole extract flow-through the anti GFP beads indicates equal loading. Right panel indicates parallel

immmunoprecipitation with anti Msp300 followed by Western with anti Msp300, indicating several high molecular weight bands.

C - A model describing the localization and putative interactions of Ma2/d with Msp300 and with Amph. Ma2/d is present at the T-tubules, and the SR membranes. It interacts with Amphiphysin at both sites. Amphiphysin interacts with Msp300 isoform lacking the KASH domain. Interactions between these proteins mediate contact sites between the T-tubule-SR-ER membranes, essential for the interactions between these organelles and the myonuclei.

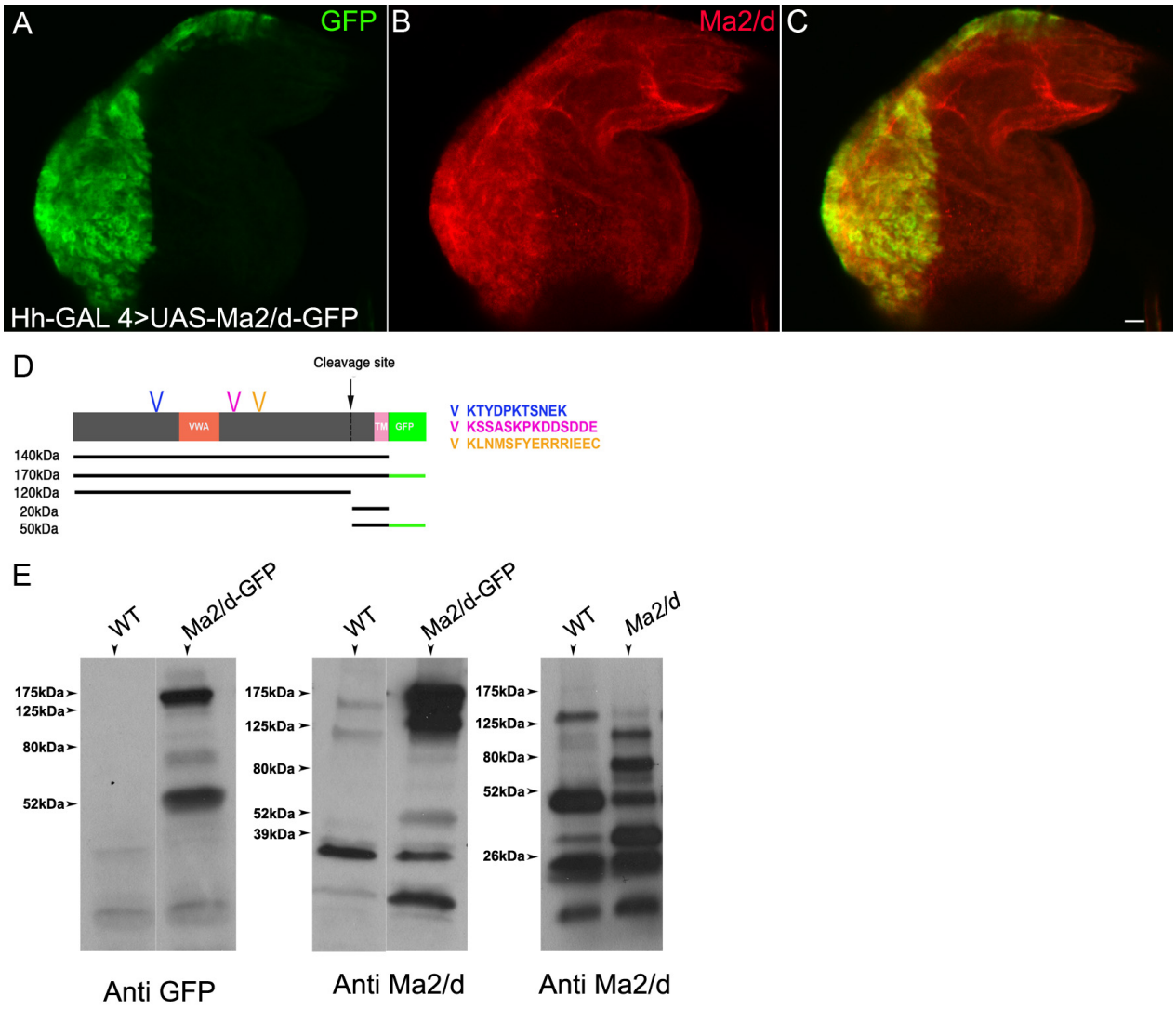

Figure S1: Verification of anti Ma2/d specificity

A-C: Wing imaginal disc of larvae over expressing Ma2/d-GFP driven by Hh-GAL4, labeled with anti GFP (A) and anti Ma2/d anibody raised against 3 peptides (marked in D) of the extracellular domain of Ma2/d, indicating that the antibody recognizes the Ma2/d. (E) Western analysis: Left panel - Western blot of larval protein extract from wild type (WT) or larvae expressing Ma2/d-GFP in muscles (driven by mef2-GAL4) reacted with anti GFP. Two specific bands representing un-cleaved Mα2δ-GFP

(~170kDa) and cleaved Ma2/d-GFP (~ 50kDa) are shown; The anti GFP is not expected to recognize the cleaved 120kDa polypeptide. Middle panel: Western blot of larval protein extract from WT (left lane), and larvae expressing Ma2/d-GFP in

muscles (right lane), both reacted with anti Ma2/d ab . In the lane of extract expressing Ma2/d-GFP the antibody recognizes a 170kDa band corresponding to the intact 170kDa protein and 120kDa band corresponding to the larger portion of the cleaved protein. In the wild type larvae extract this antibody recognizes a ~140kDa corresponding to endogenous non-cleaved Ma2/d, and ~120kDa band corresponding to the larger portion of the cleaved polypeptide. In both lanes, the antibody is not expected to recognize the small-cleaved polypeptide. Right panel: Western blot of protein extract from WT (left lane) and *Ma2/d* (right lane) mutant larvae both reacted with anti Ma2/d. In the WT extract lane (left lane)the 140kDa band represents non-cleaved intact Ma2/d protein, which is missing from the extract of the mutant larvae (right lane). Instead two lower molecular weight bands, absent from WT lane, appear (~100kDa and ~75kDa), presumably corresponding to the truncated Ma2/d proteins.

Figure S2: Genomic map of EPgy2^{EY2EY09750} excision

The genomic structure of *Ma2/d* is shown. The location of the original P element as well as the excised region deduced from sequence analysis is demonstrated.

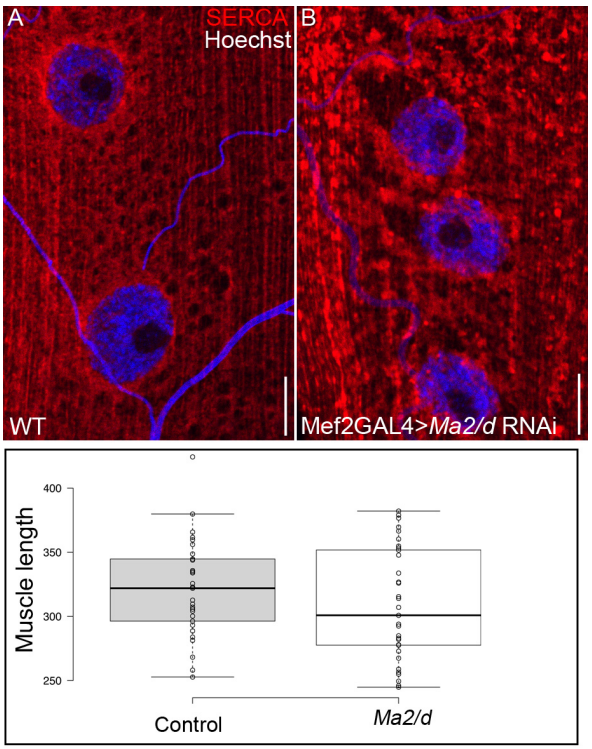

Figure S3: Aberrant nuclear position in *Ma2/d* knockdown muscles

Larval muscles of wild type (A) or larvae expressing RNAi against *Ma2/d* (B) indicating a similar phenotype of aberrant nuclear position. Bar indicates 10μm. C – quantification of *Ma2/d* larval muscle length. No significant difference between the groups is observed (*t* test: p=0.115; for WT – the length of 33 muscles (muscle 6) were measured from 4 larvae, and for *Ma2d* mutant 29 muscle (muscle 6) were measured from 4 larvae.

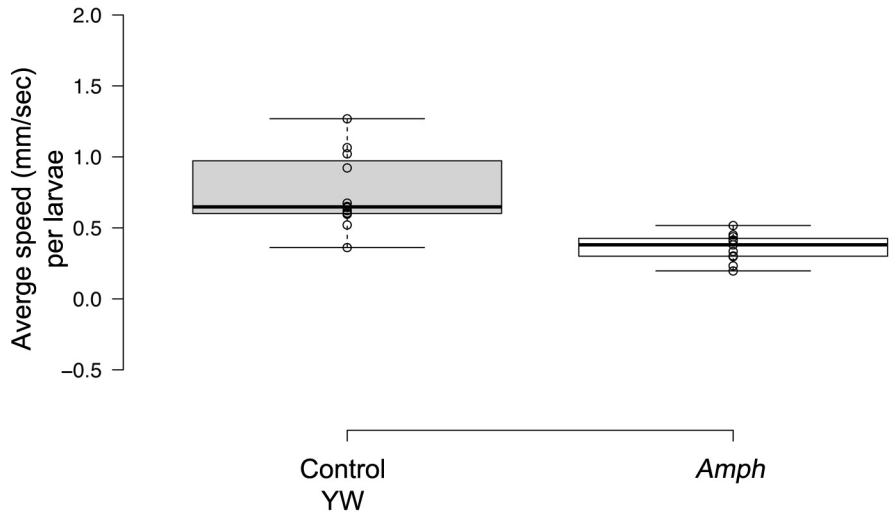

Figure S4: Locomotion assay for *Amph* mutant larvae.

Quantification of the locomotion of control (YW) and *Amph* mutant larvae. N=10 for each group .*t* -test: P<0.0002 .

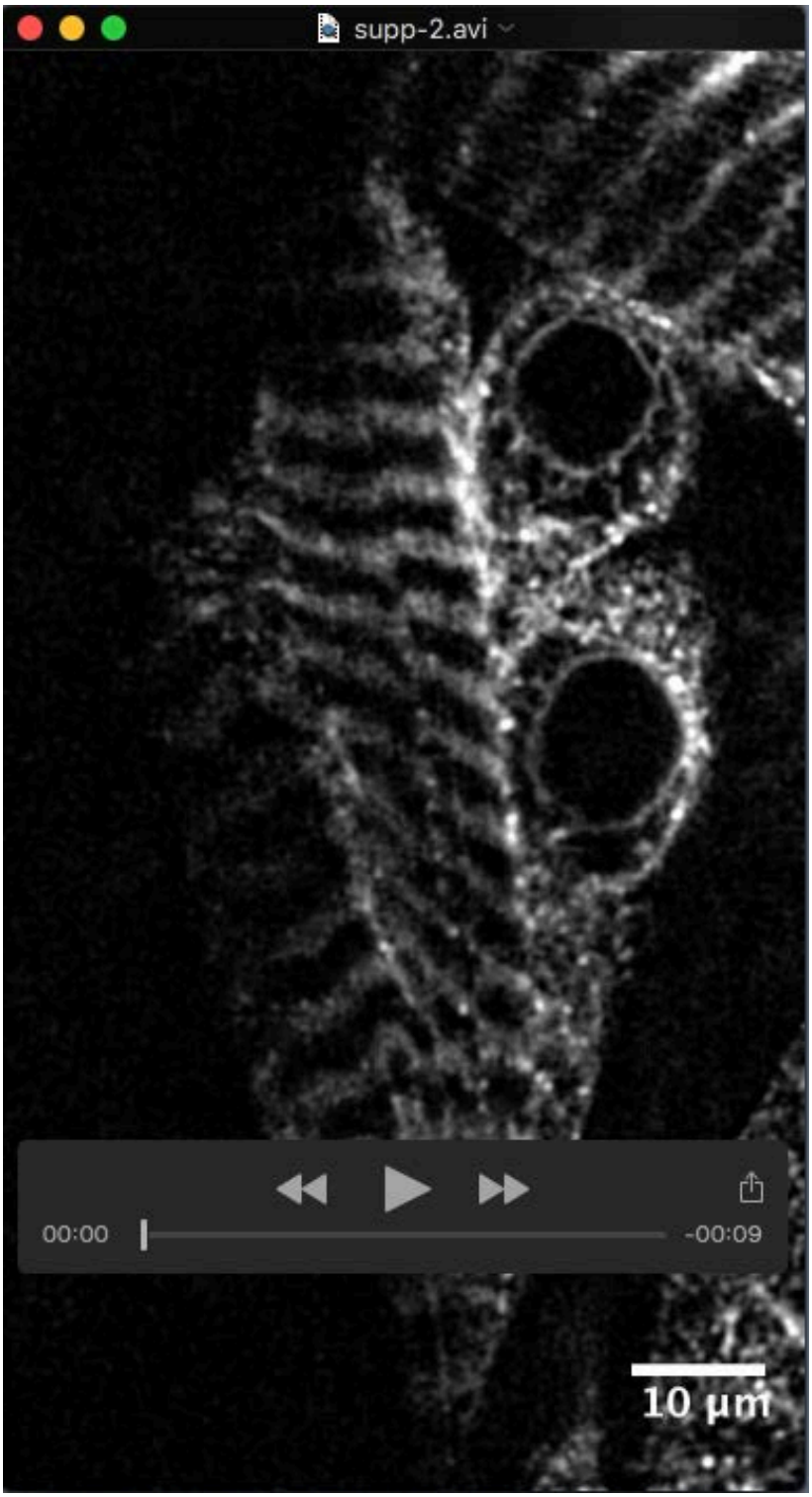

Movie S1: The distribution of Ma2/d-GFP in live 3rd instar larvae during muscle contraction imaged under Spinning disc microsope. Individual images of the movie are shown in Figure 5.

Movie S2: SERCA-Cherry distribution in live 3rd instar larvae during muscle contraction. Individual images of the movie are shown in Figure 5.

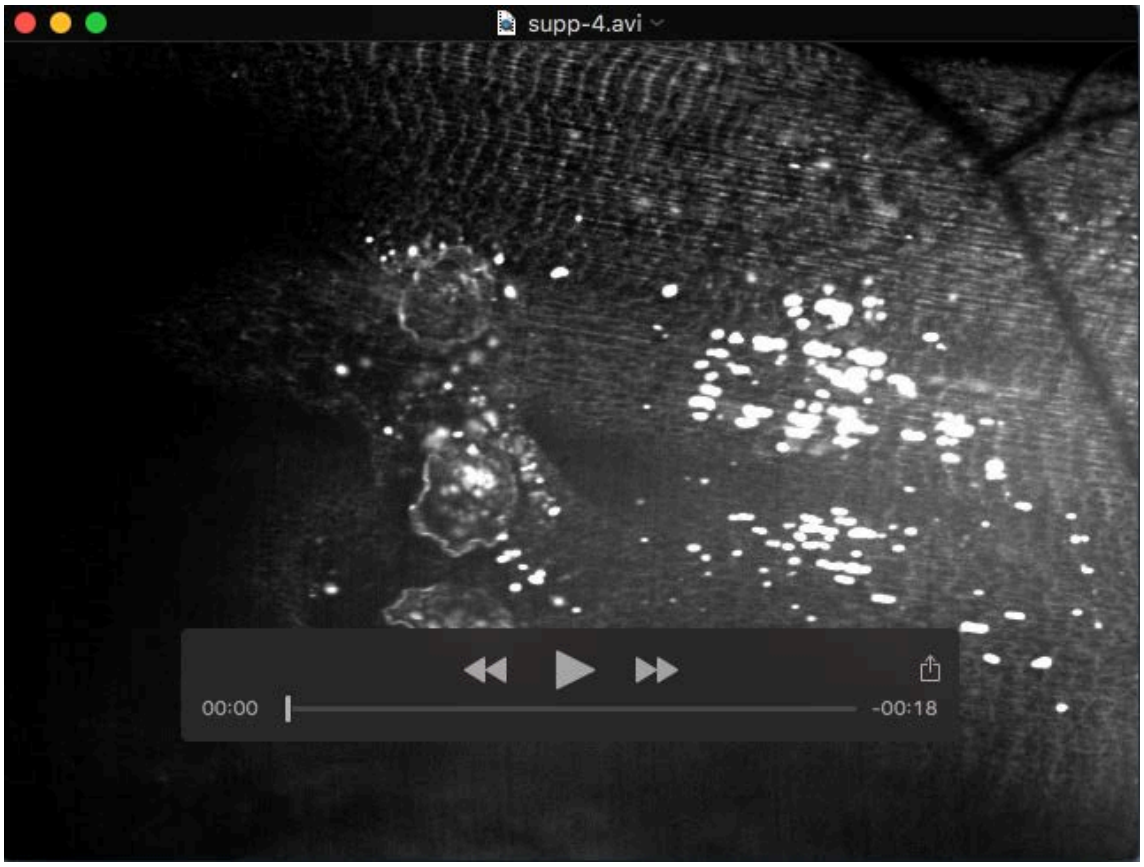

Movie S3: SERCA-Cherry distribution in live 3rd instar larvae mutant for *Ma2/d* during muscle contraction. Individual images of the movie are shown in Figure 5.